2. EXPLANATORY NOTES[1]

Shipboard Scientific Party[2]

INTRODUCTION

In this chapter, we have assembled information that will help the reader understand the basis for our preliminary conclusions and also help the interested investigator select samples for further analysis. This information concerns only shipboard operations and analyses described in the site reports in the *Initial Results* volume of the Leg 133 *Proceedings of the Ocean Drilling Program*. Methods used by various investigators for shore-based analysis of Leg 133 data will be detailed in the individual scientific contributions published in the *Scientific Results* volume.

Authorship of Site Chapters

The separate sections of the site chapters were written by the following shipboard scientists (authors are listed in alphabetical order, no seniority is necessarily implied):

Site Summary: Davies, McKenzie
Background and Objectives: Davies, McKenzie
Operations: Palmer-Julson, Pollard
Site Geophysics: Symonds
Lithostratigraphy: Brachert, Dix, Droxler, Feary, Glenn, Konishi, Martín, Montaggioni, Müller, Pigram, Watts
Basement Composition: Feary
Biostratigraphy: Betzler, Gartner, Katz, Kroon, Wei
Paleomagnetism: Khan, McNeill
Sedimentation Rates: Betzler, Gartner, Katz, Khan, Kroon, McNeill, Wei
Inorganic Geochemistry: Isern, Swart
Organic Geochemistry: Crumière
Physical Properties: Chen, Ladd, Palmer-Julson
Downhole Logging: Jackson, Jarrard
Seismic Stratigraphy: Davies, Feary, Pigram, Symonds
Summary and Conclusions: Davies, McKenzie

Following the text of each site chapter are summary core descriptions ("barrel sheets" and basement rock visual core descriptions) and photographs of each core.

Survey and Drilling Data

Geophysical survey data collected during Leg 133 falls into two categories: magnetic and bathymetric data acquired during the transit from Guam to northeastern Australia, and (2) data collected between sites. The survey data used for final site selection, including data collected during both site surveys prior to Leg 133 and short site-location surveys during Leg 133, are presented in the "Site Geophysics" section of the individual site chapters (this volume). During the Leg 133 *JOIDES Resolution* surveys, single-channel seismic, 3.5- and 12-kHz echo sounder, and magnetic data were recorded across the planned drilling sites to aid site confirmation prior to dropping a beacon.

The single-channel seismic profiling system used two 80-in^3 water guns as the energy source and a Teledyne streamer with a 100-m-long active section. These data were recorded digitally on tape using a Masscomp 561 super minicomputer and also were displayed in real time in analog format on two Raytheon recorders using a variety of filter settings (commonly 30–140 Hz) and two different scales (commonly 1- and 2-s sweeps and 50 traces/in.).

Bathymetric data collected using the 3.5- and 12-Khz precision depth recorder (PDR) system were displayed on two Raytheon recorders. Depths were calculated on the basis of an assumed 1463-m/s sound velocity in water. The water depth (in meters) at each site was corrected for (1) the variation in sound velocity with depth using Matthews' table (1939) and (2) the depth of the transducer pod (6.8 m) below sea level. In addition, depths referred to the drilling-platform level have been corrected for the height of the rig floor above the water line, which gradually increased from 10.89 to 11.41 m throughout the cruise (see Fig. 1).

Magnetic data were collected using a Geometrics 801 proton precession magnetometer, were displayed on a strip chart recorder, and were recorded on magnetic tape for later processing.

Drilling Characteristics

Because water circulation downhole is open, cuttings are lost onto the seafloor and cannot be examined. The only available information about sedimentary stratification in uncored or unrecovered intervals, other than from seismic data or wireline logging results, is from an examination of the behavior of the drill string, as observed and recorded on the drilling platform. Typically, the harder a layer, the slower and more difficult it is to penetrate. A number of other factors may determine the rate of penetration, so it is not always possible to relate the drilling time directly to the hardness of the layers. Bit weight and revolutions per minute, recorded on the drilling recorder, also influence penetration rate.

Drilling Deformation

When cores are split, many show signs of significant sediment disturbance, including the downward-concave appearance of originally horizontal bands, haphazard mixing of lumps of different lithologies (mainly at the tops of cores), and the near-fluid state of some sediments recovered from tens to hundreds of meters below the seafloor. Core deformation probably occurs during cutting, retrieval (with accompanying changes in pressure and temperature), and core handling on deck.

Shipboard Scientific Procedures

Numbering of Sites, Holes, Cores, and Samples

Drilling sites are numbered consecutively from the first site drilled by the *Glomar Challenger* in 1968. A site number refers

[1] Davies, P. J., McKenzie, J. A., Palmer-Julson, A., et al., 1991. *Proc. ODP, Init. Repts.*, 133: College Station, TX (Ocean Drilling Program).

[2] Shipboard Scientific Party is as given in list of participants preceding the contents.

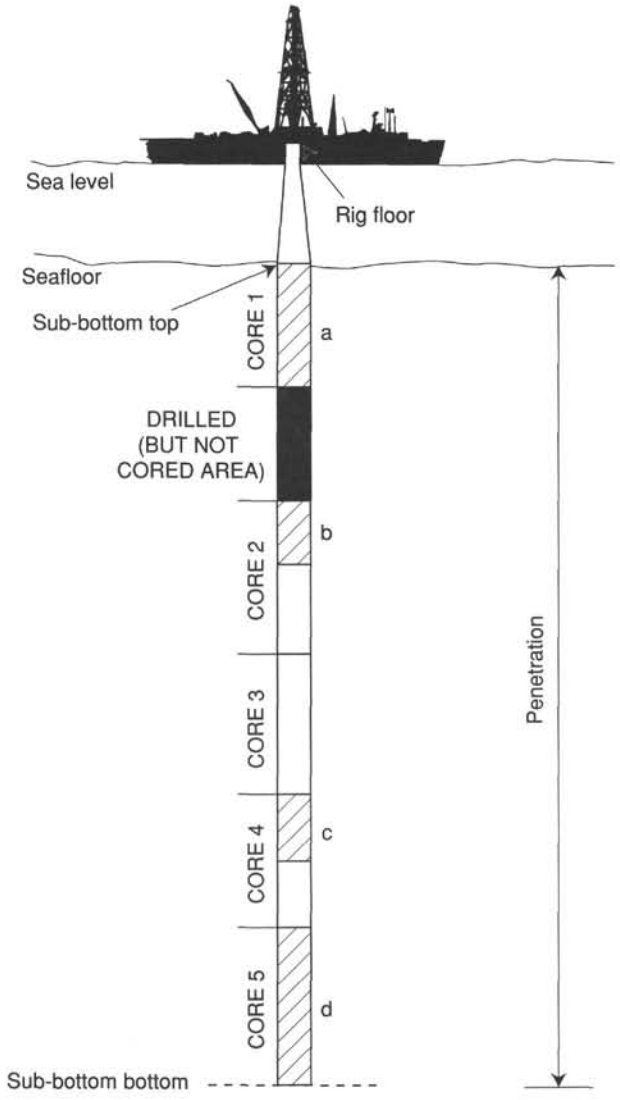

Figure 1. Diagram illustrating terms used for discussion of coring operations and core recovery.

to one or more holes drilled while the ship was positioned over one acoustic beacon. Multiple holes may be drilled at a single site by pulling the drill pipe above the seafloor (out of the hole), moving the ship some distance from the previous hole, and then drilling another hole. In some cases, the ship may return to a previously occupied site to drill additional holes (e.g., as was done for Hole 812C).

For all ODP drill sites, a letter suffix distinguishes each hole drilled at the same site. For example, the first hole drilled is assigned the site number modified by the suffix A, the second hole takes the site number and suffix B, and so forth. Note that this procedure differs slightly from that used by DSDP (Sites 1 through 624), but prevents ambiguity between site- and hole-number designations. For sampling purposes, it is important to distinguish among holes drilled at a site. Sediments or rocks recovered from different holes usually do not come from equivalent positions in the stratigraphic column, even if the core numbers are identical.

The cored interval is measured in meters below seafloor (mbsf); sub-bottom depths are determined by subtracting the drill-pipe measurement (DPM) water depth (the length of pipe from the rig floor to the seafloor) from the total DPM (from the rig floor to the bottom of the hole; see Fig. 1). Note that although the echo-sounding data (from the PDRs) are used to locate the site, they are not used as a basis for any further measurements.

The depth interval assigned to an individual core begins with the depth below the seafloor at which the coring operation began and extends to the depth at which the coring operation ended for that core (see Fig. 1). For rotary coring (RCB and XCB), each coring interval is equal to the length of the joint of drill pipe added for that interval (though a shorter core may be attempted in special instances). The drill pipe in use varies from about 9.4 to 9.8 m. The pipe is measured as it is added to the drill string, and the cored interval is recorded as the length of the pipe joint to the nearest 0.1 m. For hydraulic piston coring (APC) operations, the drill string is advanced 9.5 m, the maximum length of the piston stroke.

Coring intervals are not necessarily adjacent, but may be separated by drilled intervals. In soft sediments, the drill string can be "washed ahead" with the core barrel in place, without recovering sediments. This is achieved by pumping water down the pipe at high pressure to wash the sediment out of the way of the bit and up the annulus between the drill pipe and the wall of the hole. If thin, hard, rock layers are present, then it is possible to get "spotty" sampling of these resistant layers within the washed interval, and thus to have a cored interval greater than 9.5 m. When drilling hard rock, a center bit may replace the core barrel if it is necessary to drill without core recovery.

Cores taken from a hole are numbered serially from the top of the hole downward. Core numbers and their associated cored intervals in meters below seafloor usually are unique in a given hole; however, this may not be true if an interval must be cored twice, because of caving of cuttings or other hole problems. Maximum full recovery for a single core is 9.5 m of rock or sediment, contained in a plastic liner (6.6 cm internal diameter), plus about 0.2 m (without a plastic liner) in the core catcher (Fig. 2). The core catcher is a device at the bottom of the core barrel that prevents the core from sliding out when the barrel is being retrieved from the hole. For sediments, the core-catcher sample is extruded into a short piece of plastic liner and is treated as a separate section below the last core section. For hard rocks, material recovered in the core catcher is included at the bottom of the last section. In certain situations (e.g., when coring gas-charged sediments that ex-

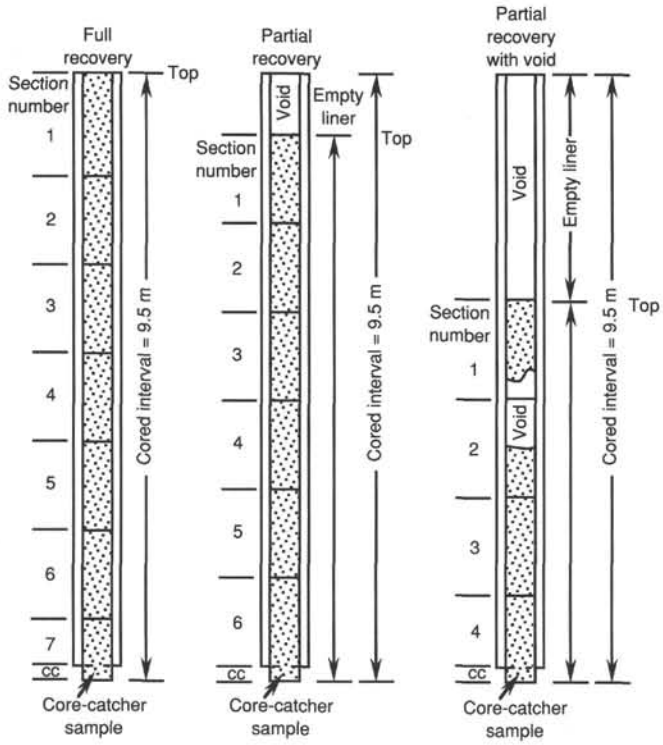

Figure 2. Diagram showing procedure used for cutting and labeling core sections.

pand while being brought on deck), recovery may exceed the 9.5-m maximum.

A recovered core is divided into 1.5-m sections, numbered serially from the top (Fig. 2). When full recovery is obtained, the sections are numbered from 1 through 7, with the last section possibly being shorter than 1.5 m (rarely, an unusually long core may require more than 7 sections). When less than full recovery is obtained, there will be as many sections as needed to accommodate the length of the core recovered; for example, 4 m of core would be divided into two 1.5-m sections and one 1-m section. If cores are fragmented (recovery less than 100%), sections are numbered serially and intervening sections are noted as void, whether shipboard scientists believe that the fragments were contiguous *in-situ* or not. In rare cases, a section of less than 1.5 m may be cut to preserve features of interest (e.g., lithological contacts).

By convention, material recovered from the core catcher is placed below the last section when the core is described and labeled core catcher (CC); in sedimentary cores, it is treated as a separate section. The core catcher is placed at the top of the cored interval in cases where material has been recovered only in the core catcher. However, information supplied by the drillers or by other sources may allow for more precise interpretation as to the correct position of core-catcher material within an incompletely recovered cored interval.

Igneous or metamorphic rock cores are also cut into 1.5-m sections, which are numbered serially; individual pieces of rock are then each assigned a number. Fragments of a single piece are assigned a single number, and individual fragments are identified alphabetically. The core-catcher sample is placed at the bottom of the last section and is treated as part of the last section, rather than separately. Scientists completing visual core descriptions describe each lithologic unit, noting core and section boundaries only as physical reference points.

When, as is usually the case, the recovered core is shorter than the cored interval, the top of the core is equated with the top of the cored interval by convention to achieve consistency in handling analytical data derived from the cores. Samples removed from the cores are designated for shore-based study, but others are analyzed immediately as part of the shipboard safety and pollution-prevention program. Next, the core is marked into section lengths, each section is labeled, and the core is cut into sections. Interstitial water (IW) and organic geochemistry (OG) samples are then taken. In addition, some headspace gas samples are scraped from the ends of cut sections on the catwalk and sealed in glass vials for light hydrocarbon analysis. Each section is then sealed at the top and bottom by gluing on color-coded plastic caps: blue to identify the top of a section and clear for the bottom. A yellow cap is placed on the section ends from which a whole-round sample has been removed, and the sample code (e.g., IW) is written on the yellow cap. The caps are usually attached to the liner by coating the end liner and the inside rim of the cap with acetone, after which the caps are taped to the liners.

The cores then are carried into the laboratory, where the sections are again labeled, using an engraver to permanently mark the full designation of the section. The length of the core in each section and the core-catcher sample are measured to the nearest centimeter; this information is logged into the shipboard CORELOG database program.

Whole-round sections from APC and XCB cores are normally run through the multisensor track (MST). The MST includes the GRAPE (gamma ray attenuation porosity evaluator) and *P*-wave logger devices, which measure bulk density, porosity, and sonic velocity, and also includes a meter to determine the volume magnetic susceptibility. At this point, whole-round samples for physical properties (PP) are taken. In well-lithified sedimentary cores, the core liner is split and the top half removed so that the whole-round core can be observed before selecting samples. Relatively soft sedimentary cores are equilibrated to room temperature (approximately 3 hr) should they be used for thermal conductivity measurements.

Cores of soft material are split lengthwise into working and or shore-based study, but others are analyzed immediately as part of the shipboard safety and pollution-prevention program. Next, the core is marked into section lengths, each section is labeled, and the core is cut into sections. Interstitial water (IW) and organic geochemistry (OG) samples are then taken. In addition, some headspace gas samples are scraped from the ends of cut sections on the catwalk and sealed in glass vials for light hydrocarbon analysis. Each section is then sealed at the top and bottom by gluing on color-coded plastic caps: blue to identify the top of a section and clear for the bottom. A yellow cap is placed on the section ends from which a whole-round sample has been removed, and the sample code (e.g., IW) is written on the yellow cap. The caps are usually attached to the liner by coating the end liner and the inside rim of the cap with acetone, after which the caps are taped to the liners.

The cores then are carried into the laboratory, where the sections are again labeled, using an engraver to permanently mark the full designation of the section. The length of the core in each section and the core-catcher sample are measured to the nearest centimeter; this information is logged into the shipboard CORELOG database program.

Whole-round sections from APC and XCB cores are normally run through the multisensor track (MST). The MST includes the GRAPE (gamma ray attenuation porosity evaluator) and *P*-wave logger devices, which measure bulk density, porosity, and sonic velocity, and also includes a meter to determine the volume magnetic susceptibility. At this point, whole-round samples for physical properties (PP) are taken.

In well-lithified sedimentary cores, the core liner is split and the top half removed so that the whole-round core can be observed before selecting samples. Relatively soft sedimentary cores are equilibrated to room temperature (approximately 3 hr) should they be used for thermal conductivity measurements.

Cores of soft material are split lengthwise into working and archive halves. Softer cores are split with a wire or saw, depending on the degree of induration. Harder cores are split with a band saw or diamond saw. The wire-cut cores are split from the bottom to top, so investigators should be aware that older material might have been transported up the core on the split face of each section.

The working half of the core is sampled for both shipboard and shore-based laboratory studies. Each extracted sample is logged into the sampling computer database program by the location and the name of the investigator receiving the sample. Records of all removed samples are kept by the curator at ODP. The extracted samples are sealed in plastic vials or bags and labeled. Samples are routinely taken for shipboard physical property analysis. These samples are subsequently used for calcium carbonate (coulometric analysis) and organic carbon (CNS elemental analyzer), and the data are reported in the site chapters.

The archive half is described visually. Smear slides are made from samples taken from the archive half and are supplemented by thin sections taken from the working half. Most archive sections are run through the cryogenic magnetometer. The archive half is then photographed using both black-and-white and color film, a whole core at a time. Close-up photographs (black-and-white) are taken of particular features for illustrations in the summary of each site, as requested by individual scientists.

Both halves of the core are then placed into labeled plastic tubes, sealed, and transferred to cold-storage space aboard the drilling vessel. Leg 133 cores were transferred from the ship in refrigerated airfreight containers to cold storage at the Gulf Coast Repository at the Ocean Drilling Program, Texas A&M University, College Station, Texas.

Igneous and Metamorphic Rocks

Igneous and metamorphic rock cores are handled differently from sedimentary cores. Once on deck, the core-catcher is placed at the bottom of the core liner, and total core recovery is calculated by shunting the rock pieces together and measuring to the nearest centimeter; this information is logged into the shipboard core-log database program. The core is then cut into 1.5-m-long sections and transferred into the laboratory.

The contents of each section are transferred into 1.5-m-long sections of split core liner, where the bottom of oriented pieces (i.e., pieces that clearly could not have rotated top-to-bottom about a horizontal axis in the liner) are marked with a red wax pencil. This is to ensure that orientation is not lost during splitting and labeling. Then, the core is split into archive and working halves. A plastic spacer is used to separate individual pieces and/or reconstructed groups of pieces in the core liner. These spacers may represent a substantial interval of no recovery. Each piece is numbered sequentially from the top of each section, beginning with number 1; reconstructed groups of pieces are assigned the same number, but are lettered consecutively. Pieces are labeled only on external surfaces. If the piece is oriented, an arrow is added to the label pointing to the top of the section.

The working half of the hard-rock core is then sampled for shipboard laboratory studies. Records of all samples are kept by the curator at ODP.

The archive half is described visually, then photographed using both black-and-white and color film, one core at a time. Both halves of the core are then shrink-wrapped in plastic to prevent rock pieces from vibrating out of sequence during transit, put into labeled plastic tubes, sealed, and transferred to cold-storage space aboard the drilling vessel. As with the other Leg 133 cores, they are housed at the Gulf Coast Repository.

VISUAL CORE DESCRIPTIONS

Visual Core Description Forms and "Barrel Sheets"

Shipboard sedimentologists describe each 1.5-m-long section of core and record their observations on visual core description forms (VCDs). Copies of VCDs are available through the ODP Data Librarian. Data recorded on the VCDs were summarized and compiled on board the ship into core-description forms, or "barrel sheets" (Fig. 3) and are published at the end of each site chapter in association with the core photographs.

Shipboard sedimentologists were responsible for visual core descriptions, smear-slide and coarse-fraction analyses, and thin-section studies of sedimentary material. Mineral-composition data were determined by X-ray diffraction, and these data augment the visual core descriptions. Data about biostratigraphy (age), geochemistry ($CaCO_3$ and C_{org}), magnetics, and physical properties (wet-bulk density and porosity) also were integrated with the sedimentologic information.

Core Designation

Core designations specify the leg, site, hole, core number, and core type, as discussed in a preceding section (see "Numbering of Sites, Holes, Cores, and Samples," this chapter). The cored interval is specified in terms of meters below seafloor (mbsf). On the basis of DPMs, which are reported by the SEDCO coring technician and the ODP operations superintendent, depths are corrected for the height of the rig floor dual elevator stool above sea level to give true water depth.

Paleontological Data

Microfossil abundances, preservation, and zone assignments appear on the core-description form under the heading "Biostrat. Zone/Fossil Character." The chronostratigraphic unit, as defined by paleontological results, is shown in the "Time-Rock Unit" column. Detailed information for the zonations, together with terms used to report abundance and preservation, are presented in the "Biostratigraphy" section (this chapter). In most cases, ages were determined for each core from core-catcher samples.

Paleomagnetic, Physical Property, and Chemical Data

Columns on the core description form display the results of paleomagnetic measurements (normal, reversed, or unknown polarity, shown as "N," "R," or "?," respectively), physical properties values (wet-bulk density and porosity) and chemical data (percentages of $CaCO_3$ determined with a coulometrics analyzer). Additional information about shipboard procedures for collecting these types of data appears in the "Paleomagnetism," "Physical Properties," and "Inorganic Geochemistry" sections (this chapter).

Graphic Lithology Column

The lithologies of the material recovered are illustrated graphically on the core description forms, either by a single pattern or by two or more patterns for mixed sediments (see

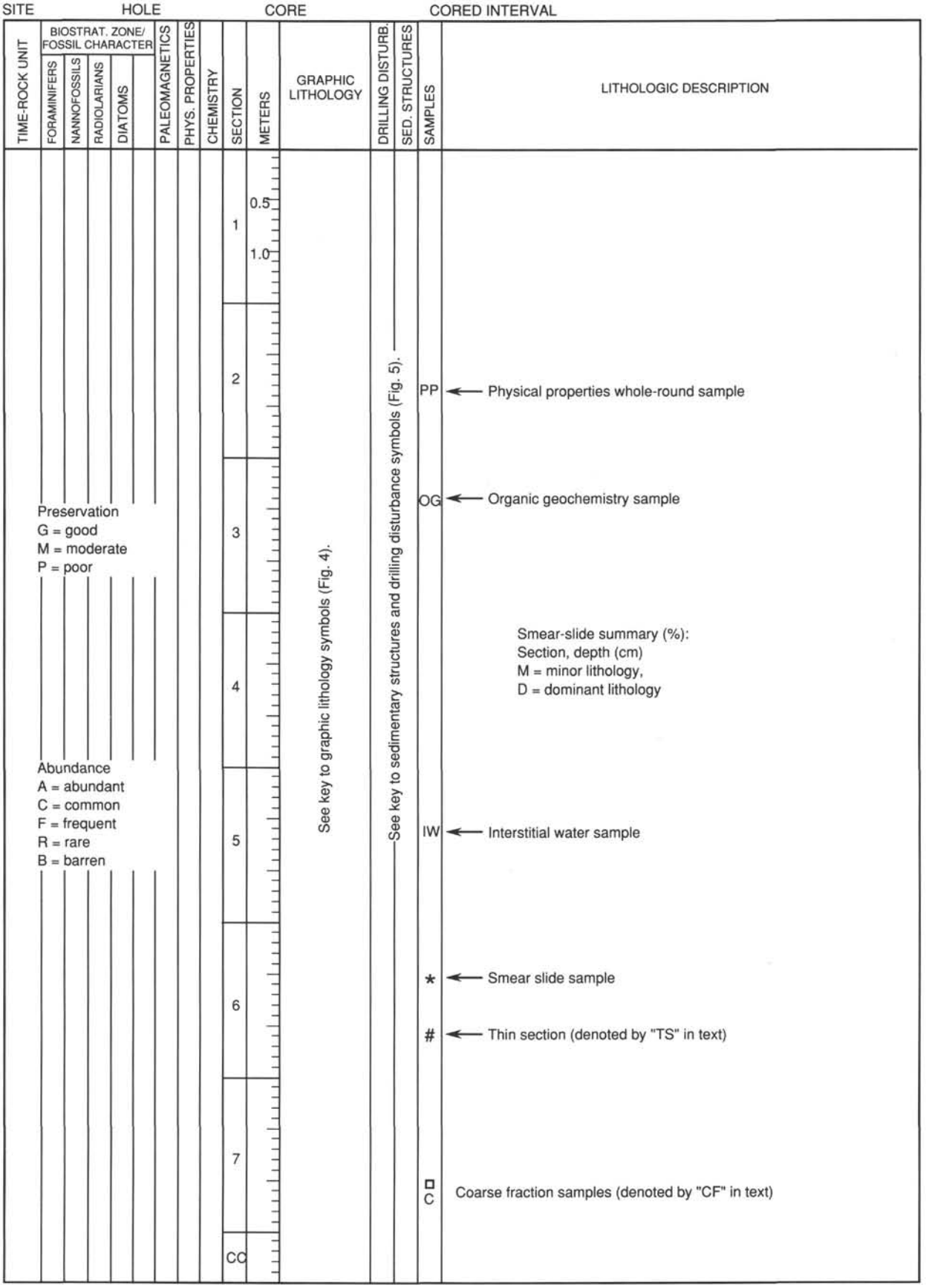

Figure 3. Core description form ("barrel sheet") used for sediments and sedimentary rocks.

Fig. 3). Where an interval of sediment or sedimentary rock is a homogeneous mixture, the constituent categories are separated by a solid vertical line, and each category is represented by its own pattern.

Only intervals exceeding 10 cm can be displayed in the graphic lithology column at the scale with which the "barrel sheets" are published in the ODP *Proceedings*. Information on finer-scale lithologic variations is included in the shipboard VCD forms, which are available from the ODP data librarian upon request.

Sedimentary Structures

In sediment cores, primary sedimentary structures (Fig. 4) can be distinguished with difficulty from structures created by the coring process. Primary sedimentary structures are illustrated by symbols in the "Sedimentary Structure" column of the core-description form. Figure 5 shows the list of the symbols used during Leg 133 to describe the primary biogenic and physical sedimentary structures. The most common types of structures include scoured basal contacts, graded beds, cross lamination, parallel laminae, and various degrees of bioturbation.

Sediment Disturbance

Sediment disturbances that clearly result from the coring process, rather than from structural deformation, are illustrated in the "Drilling Disturbance" column on the core description form (using the symbols shown in Fig. 5). Blank regions indicate the absence of drilling disturbance. Drilling disturbances for soft and firm sediments were categorized as follows:

1. Slightly deformed = bedding contacts are slightly bent.
2. Moderately deformed = bedding contacts show extreme bowing.
3. Highly deformed = bedding is completely disturbed and, in some cases, shows symmetric diapirlike structures ("flow-in").
4. Soupy = intervals are water-saturated and have lost all aspects of original bedding and primary sedimentary structures.

The degree of fracturing in indurated sediments and igneous rocks was described using the following categories:

1. Slightly fractured = core pieces are in place and contain little drilling slurry or breccia.
2. Moderately fragmented = core pieces are in place or partly displaced, but original orientation is preserved or recognizable (drilling slurry may surround fragments).
3. Highly fragmented = pieces are from the interval cored and probably in correct stratigraphic sequence (although they may not represent the entire section), but original orientation is completely lost.
4. Drilling breccia = core pieces have lost their original orientation and stratigraphic position and may be mixed with drilling slurry.

Color

Colors were determined qualitatively by comparison with Munsell Soil Color Charts (Munsell Soil Color Charts, 1971). Colors were described immediately after the cores were split because redox-associated color changes may occur when deep-sea sediments are exposed to the atmosphere. Information for core colors is given in the text of the "Lithologic Description" on the core description forms.

Samples

The positions of samples taken from each core for shipboard analyses are indicated in the "Samples" column of the core description form (Fig. 3). Locations of samples are identified in this manner: the symbol "*" indicates smear-slide samples, "TS" indicates thin-section samples, and "CF" indicates coarse-fraction samples. The notations "IW," "OG," and "PP" designate the locations of samples for whole-round interstitial-water geochemistry, frozen organic geochemistry, and physical properties, respectively.

Although not indicated in the "Samples" column, the positions of samples for routine physical property (index properties and acoustic velocity) and geochemical ($CaCO_3$ and organic carbon) analyses are indicated by dots in the "Physical Properties" and "Chemistry" columns.

Shipboard paleontologists generally use core-catcher samples for shipboard age determinations, although additional samples from other parts of the core may be examined as required. Examination of such samples may lead to the recognition of zonal boundaries in the core, as indicated in the appropriate column of the core description form (Fig. 3).

Smear-Slide Summary

A table summarizing data from smear slides and thin sections appears on each core-barrel description form. These tables include information about the sample location, whether the sample represents a dominant ("D") or a minor ("M") lithology in the core, and the estimated percentage ranges of sand, silt, and clay, together with all identified components. We emphasize here that smear slide analyses provide only crude estimates of the relative abundances of detrital constituents; the mineralogies of finer-grained particles are difficult to identify petrographically, and sand-sized grains tend to be underestimated because they cannot be incorporated into the smear evenly. In addition, estimates of grain size suffer from systematic errors because of differences between the surface areas of grains and their respective weight-percentages; this is particularly problematic with clay-sized particles. Coarse-fraction separates were made of selected samples and the wt% >63 mm was reported on the barrel sheets as "Percent Sand." The grain-size distributions were used to help place textural descriptions within the Shepard (1954) textural classification (Fig. 6).

Lithologic Description–Text

The lithologic descriptions that appear on each core-description form (barrel sheet) consist of two parts: (1) a brief summary of the major lithologies in the core (see "Sediment Classification" section, this chapter), followed by a description of sedimentary structures and features; and (2) a description of minor lithologies observed in the core (where present), including data about color, occurrence in the core, and significant features.

SEDIMENTOLOGY

The different core lithologies drilled during Leg 133 were described on the basis of a modified sediment classification scheme proposed by the Ocean Drilling Program (Mazzullo et al., 1987). Leg 133 classification has kept the two basic sediment and rock types described in Mazzullo et al. (1987) as (I) granular and (II) chemical sediments and rocks.

The granular sediments and rocks were subdivided in two lithologic groups: (1) the calcareous lithologies and (2) the siliceous lithologies. The calcareous and siliceous lithologies were then separated into two classes: (A) pelagic and (B)

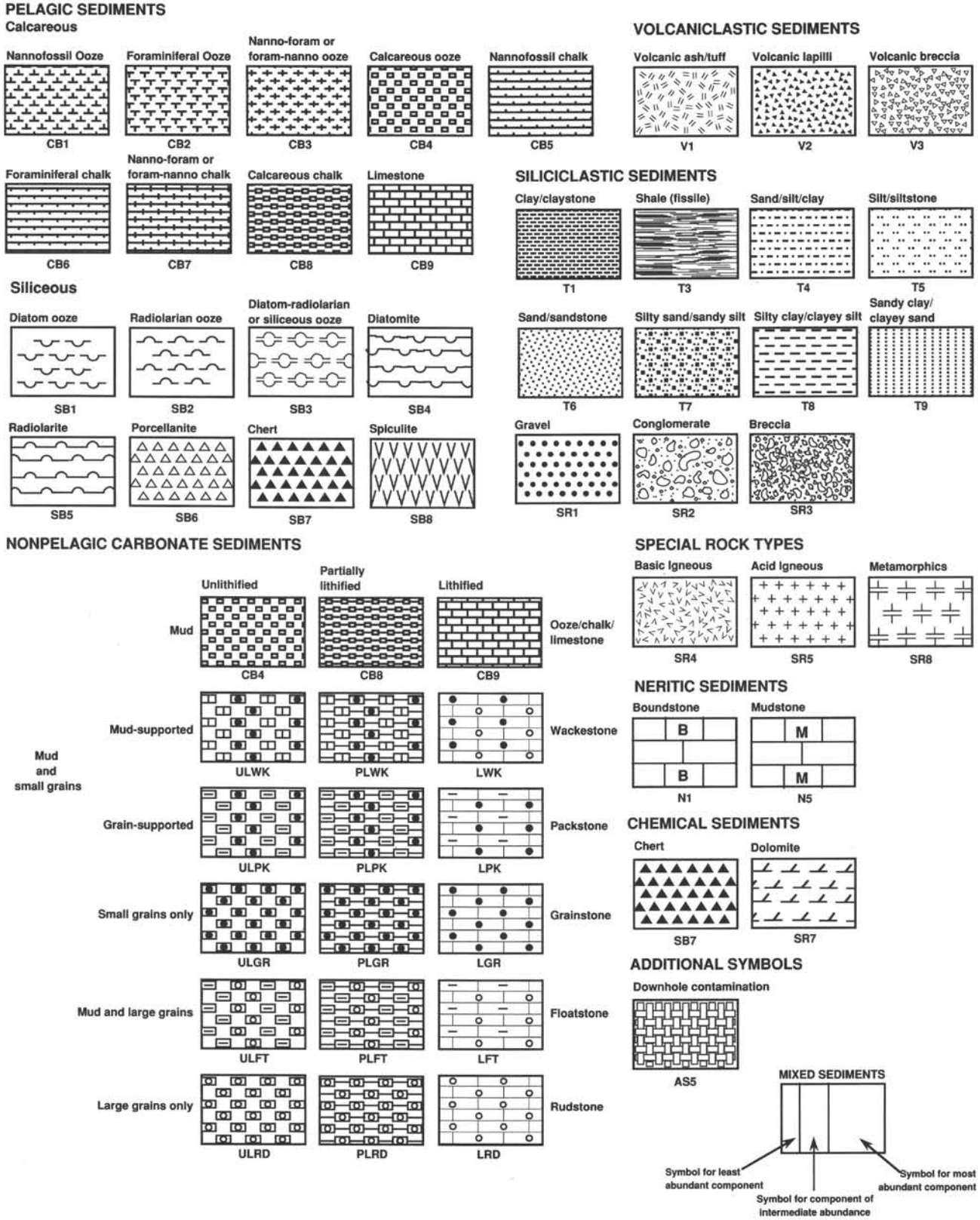

Figure 4. Key to symbols used in the "Graphic lithology" column on core description form shown in Figure 3.

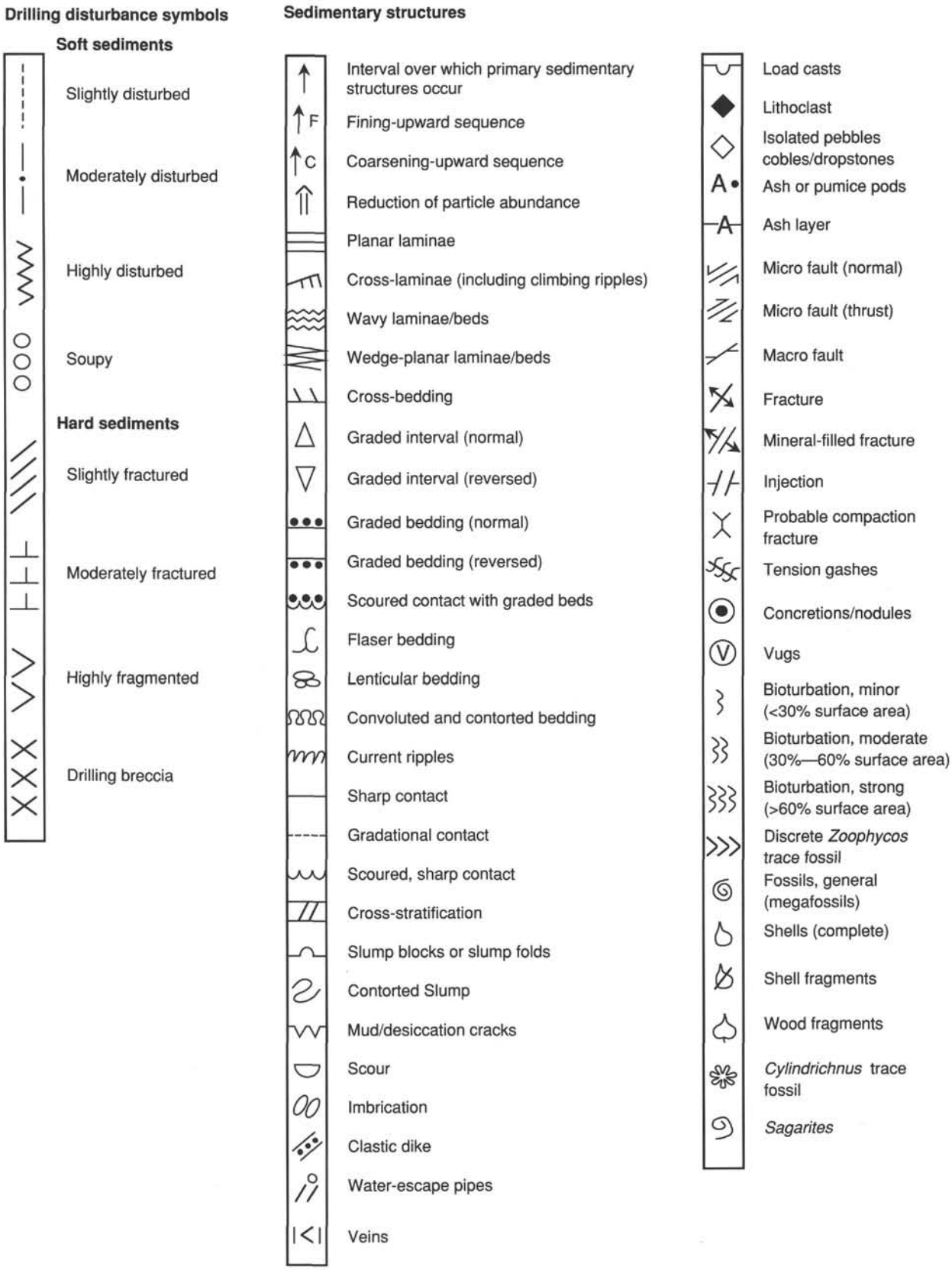

Figure 5. Symbols for drilling disturbance and sedimentary structure used on core description forms shown in Figure 3.

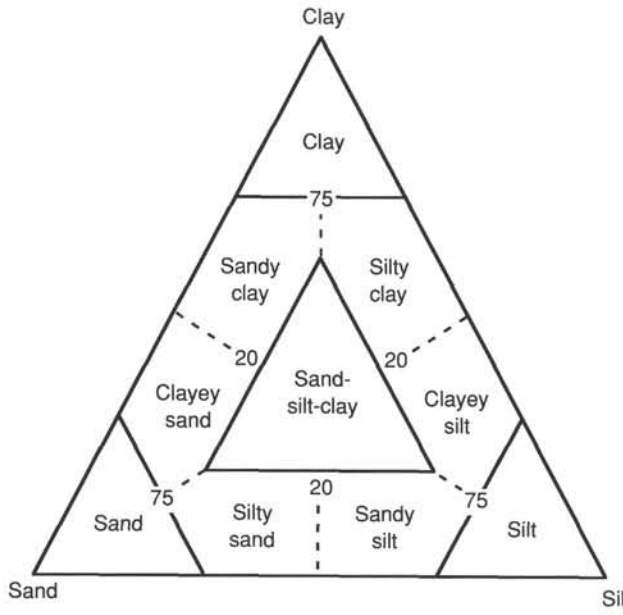

Figure 6. Ternary diagram showing principal names for siliciclastic sediments (from Shepard, 1954).

nonpelagic sediments and rocks. Finally, the nonpelagic siliceous class is subdivided in two subclasses: (a) the siliciclastics and (b) the volcaniclastics.

Classes of Granular Sediments and Rocks

Five grain types occur in granular sediments and rocks: (1) pelagic calcareous, (2) siliceous particles, (3) nonpelagic calcareous, (4) siliciclastic, and (5) volcaniclastic particles; their definitions are as follows:

1. Pelagic grains are fine-grained skeletal debris produced mainly within the upper part of the water column in open-marine environments by:

A. calcareous microfauna and microflora (e.g., foraminifers, pteropods, and nannofossils, and associated organisms) and

B. siliceous microfauna and microflora (e.g., radiolarians, diatoms, and associated organisms).

2. Nonpelagic grains are coarse- to fine-grained particles deposited in hemipelagic and nearshore environments as:

A. calcareous skeletal and nonskeletal grains and fragments (e.g., bioclasts, peloids, micrite). Note that the term micrite is used to define very fine calcareous particles (~<10 m), with no clear identification of origin observed in smear slides. These particles can be either recrystallized nannofossils or nonpelagic bank-derived calcareous mud in pelagic lithologies;

B. siliceous clastic grains comprising minerals and rock fragments that were eroded from plutonic, sedimentary, and metamorphic rocks; C. siliceous clastic grains comprising glass shards, rock fragments, and mineral crystals that were produced by volcanic processes.

Variations in the relative proportions of these five grain types define five major classes of granular sediments and rocks: (1) calcareous and siliceous pelagic, (2) nonpelagic calcareous, (3) siliciclastic, (4) volcaniclastic, and (5) mixed sediments and rocks.

Pelagic sediments and rocks contain 60% or more pelagic grains and 40% or less nonpelagic calcareous, siliciclastic, and volcaniclastic grains. Nonpelagic calcareous sediments and rocks include 60% or more nonpelagic calcareous grains and 40% or less pelagic plus nonpelagic siliciclastic and volcaniclastic grains. Siliciclastic sediments and rocks are composed of 60% or more siliciclastic grains and 40% or less pelagic plus nonpelagic calcareous and volcaniclastic grains. Volcaniclastic sediments and rocks contain 60% or more volcaniclastic grains and 40% or less pelagic plus nonpelagic calcareous and siliciclastic grains. Volcaniclastics include epiclastic sediments (eroded from volcanic rocks by wind, water, or ice), pyroclastic sediments (products of explosive magma degassing), and hydroclastic sediments (granulation of volcanic glass by steam explosions). Last, mixed sediments and rocks are composed of 40% to 60% nonpelagic calcareous, siliciclastic, and volcaniclastic grains and 40% to 60% calcareous plus siliceous pelagic grains.

Classification of Granular Sediments and Rocks

Sediment and rock names were defined solely on the basis of composition and texture. Composition becomes most important for description of those deposits more characteristic of open-marine (pelagic) conditions, with texture becoming more significant for the classification of hemipelagic and nearshore (nonpelagic) facies. Data for composition and texture of cored sediments and rocks were primarily determined aboard ship by (1) unaided visual observation, (2) visual observation using hand lens, and (3) visual estimates in smear slides, thin sections, and coarse fractions with the aid of a microscope. Calcium carbonate content was qualitatively estimated in smear slides and quantitatively estimated with coulometric analyses (see "Inorganic Geochemistry" section, this chapter). Other geologic features determined were color and firmness. Colors of the recovered material were determined with Munsell Soil Color Charts (1971). Colors were evaluated immediately after the cores were split and while they were still wet.

Firmness

The determination of induration is highly subjective, and the categories used during Leg 133 (after Gealy et al., 1971) are thought to be practical and significant. Three classes of firmness for calcareous sediments and rocks were recognized:

1. Unlithified: soft sediments that have little strength and are readily deformed under the pressure of a fingernail or the broad blade of a spatula. This corresponds to the term *ooze* for pelagic calcareous sediments. In nonpelagic calcareous sediments, the prefix *unlithified* is used (e.g., unlithified packstone).

2. Partly lithified: firm and friable sediments that can be scratched with a fingernail or the edge of a spatula blade. This corresponds to the term *chalk* for pelagic calcareous materials. In nonpelagic calcareous sediment, the prefix *partly lithified* is used (e.g., partly lithified grainstone).

3. Lithified: hard, nonfriable cemented rock, difficult or impossible to scratch with a fingernail or the edge of a spatula. This corresponds to the term *limestone* (lithified ooze) for pelagic calcareous material. In nonpelagic calcareous material, the prefix *lithified* is used (e.g, lithified floatstone).

Only two classes of firmness are used for *siliceous sediments and rocks*:

1. Soft: sediment core can be split with a wire cutter. Soft terrigenous sediment, pelagic clay, and transitional calcareous sediments are termed sand, silt, or clay.

2. Hard: the core is hard (i.e., consolidated or well indurated) if it must be cut with a hand or diamond saw. For these

<table>
<tr><td colspan="6">Allochthonous limestones
original components not organically
bound during depostion</td><td colspan="3">Autochthonous limestones
original components organically
bound during depostion</td></tr>
<tr><td colspan="4">Less than 10% > 2 mm components</td><td colspan="2">Greater than
10% > 2 mm
components</td><td colspan="3">Boundstone</td></tr>
<tr><td colspan="3">Contains lime mud (< 0.03 mm)</td><td>No
lime
mud</td><td rowspan="3">Matrix
supported</td><td rowspan="3">> 2 mm
component
supported</td><td rowspan="3">By
organisms
which
act as
barriers</td><td rowspan="3">By
organisms
which
encrust
and
bind</td><td rowspan="3">By
organisms
which
build
a rigid
framework</td></tr>
<tr><td colspan="2">Mud supported</td><td colspan="2" rowspan="2">Grain
supported</td></tr>
<tr><td>Less than
10% grains
(> 0.03 mm
to < 2 mm)</td><td>Greater
than
10%
grains</td></tr>
<tr><td>Mudstone</td><td>Wackestone</td><td>Packstone</td><td>Grainstone</td><td>Floatstone</td><td>Rudstone</td><td>Bafflestone</td><td>Bindstone</td><td>Framestone</td></tr>
</table>

Figure 7. The Dunham (1962) classification of limestones according to depositional texture, as modified by Embry and Klovan (1971).

materials, the suffix "*-stone*" is added to the soft-sediment name (e.g., sandstone, siltstone, and claystone). Note that this varies from terms used to described nonpelagic calcareous sediments, for which the suffix "*- stone*" has no firmness implications (e.g., wackestone, packstone, etc.).

X-Ray Diffraction

The mineralogy and relative abundances of common minerals were analyzed for bulk samples using X-ray diffraction techniques (See "Inorganic Geochemistry" section, this chapter).

Principal Names

We classified granular sediment during Leg 133 by designating a principal name and major and minor modifiers. The principal name of a granular sediment defines its granular-sediment class; the major and minor modifiers describe the texture, composition, fabric, and/or roundness of the grains themselves.

Each granular-sediment class has a unique set of principal names. For pelagic sediments and rocks, the principal name describes the composition and degree of consolidation using the following terms:

1. *Ooze:* unconsolidated calcareous and/or siliceous pelagic sediment;
2. *Chalk:* firm pelagic sediment composed predominantly of calcareous pelagic grains;
3. *Limestone:* hard pelagic sediment composed predominantly of calcareous pelagic grains;
4. *Radiolarite*, *diatomite*, and *spiculite:* firm pelagic sediment composed predominantly of siliceous radiolarians, diatoms, and sponge spicules, respectively;
5. *Porcellanite:* a well-indurated rock with abundant authigenic silica but not as hard, lustrous, or brittle as chert (in part, such rocks may represent mixed sedimentary rock); and
6. *Chert:* vitreous or lustrous, conchoidally fractured, highly indurated rock composed predominantly of authigenic silica.

The principal name describes the texture and fabric, using the amplification of the original Dunham (1962) classification for nonpelagic calcareous sediments and rocks, according to depositional texture by Embry and Klovan (1971; Fig. 7). The following terms apply:

1. *Mudstone:* mud-supported fabric, with less than 10% grains, grains <2 mm in size;
2. *Wackestone:* mud-supported fabric, with greater than 10% grains, grains <2 mm in size;
3. *Packstone:* grain-supported fabric, with intergranular mud, grains <2 mm in size;
4. *Grainstone:* grain-supported fabric, no mud, grains <2 mm in size;
5. *Floatstone:* matrix-supported fabric, grains >2 mm in size;
6. *Rudstone:* grain-supported fabric, grains >2 mm in size;
7. *Boundstone:* components organically bound during deposition;
8. *Bafflestone:* formed by organisms that act as baffles;
9. *Bindstone:* formed by organisms that encrust and bind; and
10. *Framestone:* formed by organisms that build a rigid framework.

For siliciclastic sediments, texture provides the main criterion for selection of a principal name. The Udden-Went-

Millimeters	μm	Phi (Ø)	Wentworth size class	
		-20		
4096		-12	Boulder (-8 to -12 Ø)	
1024		-10		
256		-8		Gravel
64		-6	Cobble (-6 to -8 Ø)	
16		-4	Pebble (-2 to -6 Ø)	
4		-2		
3.36		-1.75		
2.83		-1.50	Granule	
2.38		-1.25		
2.00		-1.00		
1.68		-0.75		
1.41		-0.50	Very coarse sand	
1.19		-0.25		
1.00		0.00		
0.84		0.25		
0.71		0.50	Coarse sand	
0.59		0.75		
1/2 — 0.50	500	1.00		
0.42	420	1.25		
0.35	350	1.50	Medium sand	Sand
0.30	300	1.75		
1/4 — 0.25	250	2.00		
0.210	210	2.25		
0.177	177	2.50	Fine sand	
0.149	149	2.75		
1/8 — 0.125	125	3.00		
0.105	105	3.25		
0.088	88	3.50	Very fine sand	
0.074	74	3.75		
1/16 — 0.0625	63	4.00		
0.0530	53	4.25		
0.0440	44	4.50	Coarse silt	
0.0370	37	4.75		
1/32 — 0.0310	31	5		Mud
1/64 0.0156	15.6	6	Medium silt Fine silt	
1/128 0.0078	7.8	7	Very fine silt	
1/256 — 0.0039	3.9	8		
0.0020	2.0	9		
0.00098	0.98	10		
0.00049	0.49	11	Clay	
0.00024	0.24	12		
0.00012	0.12	13		
0.00006	0.06	14		

Figure 8. Udden-Wentworth grain-size classification of terrigenous sediments (from Wentworth, 1922).

worth grain-size scale (Fig. 8) defines the grain-size ranges and the names of the textural groups (*gravel*, *sand*, *silt*, and *clay*) and subgroups (*fine sand*, *coarse silt*, etc.). When two or more textural groups or subgroups are present, the principal names appear in order of increasing abundance. However, distinctions between some of the categories are dubious without accurate measurements of weight percentages. This is particularly true for the boundary between silty clay and clayey silt. The suffix "*-stone*" is affixed to the principal names sand, silt, and clay when the sediment is lithified. The terms "*conglomerate*" and "*breccia*" are the principal names of gravels having well-rounded and angular clasts, respectively.

For volcaniclastic sediments, the principal name is also dictated by the texture. The names and ranges of three textural groups (from Fisher and Schmincke, 1984) are as follows:

1. *Volcanic breccia:* pyroclasts greater than 64 mm in diameter;
2. *Volcanic lapilli:* pyroclasts between 2 and 64 mm in diameter (when lithified, the term "lapillistone" is used);
3. *Volcanic ash:* pyroclasts less than 2 m in diameter (when lithified, the term "tuff" is used).

For mixed sediments and rocks, the principal name describes the degree of consolidation, while the term *mixed sediments* is used for unlithified sediment, and the term *mixed sedimentary rock* is used for lithified sediment.

At several sites drilled during Leg 133 (particularly in the Pliocene-Pleistocene interval), we observed sediments containing pelagic calcareous grains (e.g., foraminifers, pteropods, and coccoliths) mixed with nonpelagic calcareous grains (e.g., most likely bank-derived, fine-grained aragonite and magnesian calcite particles). This nonpelagic component evidently was produced on carbonate platforms, transported offshore as suspended load during major storms, and subsequently settled through the water column along with the pelagic particles. Following the description of Schlager and James (1978), these mixed sediments were called *periplatform oozes* and *chalks*, but only after X-ray diffraction analysis to confirm the presence of aragonite and/or magnesian calcite. If fine calcareous particles were observed in addition to nannofossils in smear slides without the occurrence of aragonite and magnesian calcite (based upon X-ray diffraction analyses), the term *micrite* was used as a major (25%–40%) or minor (10%–25%) modifier. Sediment and rock having no obvious pelagic calcareous particles, but a large proportion of micrite then should be classified (using the Dunham classifications) as either a mudstone or a packstone according to the proportion of grains.

Major and Minor Modifiers

To describe the lithology of the granular sediments and rocks in greater detail, the principal name of a granular-sediment class is preceded by major modifiers and followed by minor modifiers (Table 1). Minor modifiers are preceded by the term "with." The most common uses of major and minor modifiers are to describe the composition and textures of grain types that are present in major (25%–40%) and minor (10%–25%) proportions. In addition, major modifiers can be used to describe grain fabric, grain shape, and sediment color.

The composition of pelagic grains can be described in greater detail with the major and minor modifiers *nannofossil*, *foraminifer(-al)*, *calcareous*, *diatom(-aceous)*, *radiolarian*, *spicule(-ar)*, and *siliceous*. The terms *calcareous* and *siliceous* are used to describe sediments that are composed of calcareous or siliceous pelagic grains of uncertain origin.

The compositional terms for nonpelagic calcareous grains include the following major and minor modifiers as skeletal and nonskeletal grains:

1. *Bioclast* (or *bioclastite*): fragment of skeletal remains (specific names such as molluscan or algal can also be used);
2. *Ooid* (or *oolite*): spherical or elliptical nonskeletal particles smaller than 2 mm in diameter, having a central nucleus surrounded by a rim having concentric or radial fabric;
3. *Pisolite:* spherical or ellipsoidal nonskeletal particle, commonly greater than 2 mm in diameter, with or without a central nucleus, but displaying multiple concentric layers of carbonate;
4. *Pellet* (*-al*): fecal particles from deposit-feeding organisms;
5. *Peloid* (*pel*): micritized carbonate particle of unknown origin;

Table 1. Lithologic description of granular sediments and rocks, including major and minor modifiers.

Sediment class	Major modifiers	Principal names	Minor modifiers
Pelagic sediment	1. Composition of pelagic and NPC grains present in major amounts 2. Texture of clastic grains present in major amounts	1. Ooze 2. Chalk 3. Limestone 4. Radiolarite 5. Diatomite 6. Spiculite 7. Porcellanite 8. Chert	1. Composition of pelagic and NPC grains present in minor amounts. 2. Texture of clastic grains present in minor amounts.
NPC sediment	1. Composition of NPC and pelagic grains present in major amounts 2. Texture of clastic grains present in major amounts	1. Boundstone 2. Grainstone 3. Packstone 4. Wackestone 5. Floatstone 6. Rudstone	1. Composition of NPC and pelagic grains present in minor amounts. 2. Texture of clastic grains present in minor amounts.
Siliclastic sediment	1. Composition of all grains present in major amounts 2. Grain fabric (gravels only) 3. Grain shape (optional) 4. Sediment color (optional)	1. Gravel 2. Sand 3. Silt 4. Clay (etc.)	1. Composition of all grains present in minor amounts. 2. Texture and composition of siliciclastic grains present as matric (for coarse-grain clastic sediments).
Volcaniclastic sediment	1. Composition of all volcaniclasts present in major amounts 2. Composition of all pelagic and NPC grains 3. Texture of siliciclastic grains present in major amounts	1. Breccia 2. Lapilli 3. Ash/tuff 4. Volcanic and (etc.)	1. Composition of all volcaniclastics present in minor amounts. 2. Composition of all NPC and pelagic grains present in minor amounts. 3. Texture of siliciclastic grains present in minor amounts.
Mixed sediment	1. Composition of NPC and pelagic grains present in major amounts 2. Texture of clastic grains present in major amounts	1. Mixed sediments	1. Composition of NPC and pelagic grains present in minor amounts. 2. Texture of clastic grains present in minor amounts.

Note: NPC = nonpelagic carbonate.

6. *Intraclast:* reworked carbonate-sediment/rock fragment or rip-up clast consisting of the same lithology as the host sediment;

7. *Lithoclast:* reworked carbonate-rock fragment consisting of a lithology different from the host sediment;

8. *Calcareous*, *dolomitic*, *aragonitic*, *sideritic:* the mineral composition of carbonate muds or mudstones (micrite) of nonpelagic origins.

The textural designations for siliciclastic grains utilize standard major and minor modifiers such as *gravel*(*-ly*), *sand*(*-y*), *silt*(*-y*), and *clay*(*-ey*) (Shepard, 1954). The character of siliciclastic grains can be described further by mineralogy (using modifiers such as "quartz," "feldspar," "glauconite," "mica," "kaolinite," "zeolitic," "lithic," "calcareous," "gypsiferous," or "sapropelic." In addition, the provenance of rock fragments (particularly in gravels, conglomerates, and breccias) can be described by modifiers such as volcanic, sed-lithic, meta-lithic, gneissic, and plutonic. The fabric of a sediment can also be described using major modifiers such as grain-supported, matrix-supported, and imbricated. Generally, fabric terms are useful only when describing gravels, conglomerates, and breccias.

The composition of volcaniclastic grains is described by the major and minor modifiers *lithic* (rock fragments), *vitric* (glass and pumice), and *crystal* (mineral crystals). Modifiers can also be used to describe the compositions of the lithic grains and crystals (e.g., *feldspathic* or *basaltic*).

Classes of Chemical Sediments and Rocks

Chemical sediments are composed of minerals that formed by inorganic processes such as precipitation from solution or colloidal suspension, deposition of insoluble precipitates, or recrystallization. Chemical sediments generally have a crystalline (i.e., nongranular) texture. Five classes of chemical sediments are distinguished: (1) *carbonaceous* sediments and rocks, (2) *evaporites*, (3) *silicates*, (4) *carbonates*, and (5) *metalliferous* sediments and rocks.

Carbonaceous sediments and rocks contain >50% organic matter (plant and algal remains) that has been altered from its original form by carbonization, bituminization, or putrification. Examples of carbonaceous sediments include peat, coal, and sapropel. The *evaporites* are classified according to their mineralogy using names such as halite, gypsum, and anhydrite. They may be modified by terms that describe their structure or fabric, such as massive, nodular, and nodular-mosaic. *Silicates* and *carbonates* are defined as crystalline sedimentary rocks that are nongranular and nonbiogenic in appearance. They are classified according to their mineralogy, using principal names such as chert (microcrystalline quartz), calcite, and dolomite. They should also be modified with terms that describe their crystalline (as opposed to granular) nature, such as crystalline, microcrystalline, massive, and amorphous. *Metalliferous* sediments and rocks are nongranular, nonbiogenic sedimentary rocks that contain metal-bearing minerals such as pyrite, goethite,

manganese, chamosite, and glauconite. They are classified according to their mineralogy.

BIOSTRATIGRAPHY

Preliminary age assignments were established primarily with core-catcher samples. Samples from within the cores were examined when a refined age determination was necessary. Three microfossil groups were examined for biostratigraphic purposes: calcareous nannofossils, planktonic foraminifers, and larger benthic foraminifers. Both larger and smaller foraminifers were used to estimate paleobathymetry. Sample positions and the abundance, preservation, and age or zone for each fossil group is recorded on barrel sheets for each core.

The time scale by Berggren et al. (1985a, 1985b) was used for the Cenozoic. Figures 9 and 10 summarize the nannofossil and planktonic foraminifer datums, respectively, used for Leg 133. The subdivision of Chaproniere (1981) was used for the larger benthic foraminifers.

Calcareous Nannofossils

All datable sediments and sedimentary rocks recovered during Leg 133 are of Cenozoic age. The two widely used nannofossil zonations of the Cenozoic are comparably accurate; however, numerous biohorizons have been documented that are not incorporated into either of these zonations. All available biohorizons were used to date Leg 133 sediments, often to a much greater accuracy than is possible with formal zonations alone.

Chronological Framework

The age estimates of Cenozoic calcareous nannofossil biohorizons have been derived from the geomagnetic polarity time-scale (GPTS) of Berggren et al. (1985a; 1985b; Fig. 9). Most age estimates have been taken directly from Berggren et al. (1985b). Some were modified slightly, based on more recent and more accurate dates; several additional datum levels have been included where appropriate (i.e., datums not listed by Berggren et al., 1985b).

Cenozoic Zonation

In keeping with tradition, ages also have been presented in a zonal framework. For convenience, we used the zonation of Okada and Bukry (1980), although this zonation is readily convertible to the alternative scheme of Martini (1971). Those who do not need the security of a "zonation" may wish to avail themselves of the more accurate and more precise biostratigraphy and chronostratigraphy derived from the entire spectrum of known or available biohorizons and datum levels, although this may require a slightly greater effort.

The criteria that best define late Cenozoic epoch boundaries are not necessarily the most readily identified or most easily used for shipboard determination. Consequently, a more practical, albeit somewhat arbitrary, definition of epoch boundaries was used. Because calcareous nannofossils were usually the first source for shipboard biostratigraphy, these were also the first choice for designating epoch boundaries.

The Pleistocene/Pliocene boundary was identified by the highest occurrence of *Discoaster brouweri*.

The late Pliocene and early Pliocene were separated at the highest occurrence of *Reticulofenestra pseudoumbilica*.

The Pliocene/Miocene boundary was identified by the highest occurrence of *Discoaster quinqueramus*.

The late Miocene and middle Miocene were separated at the highest occurrence of *Discoaster hamatus*.

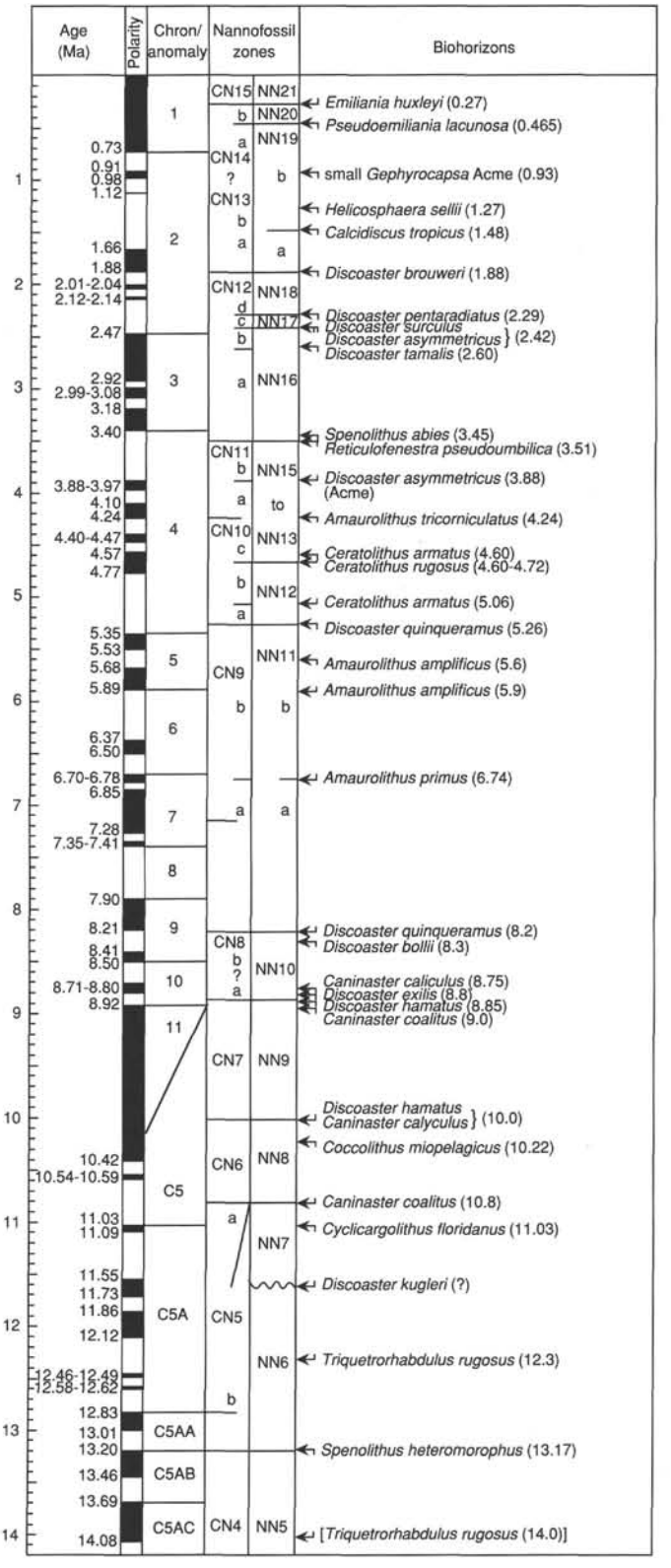

Figure 9. Nannofossil ages determined by cross-correlating with the GPTS correlation charts assembled for calcareous nannofossils.

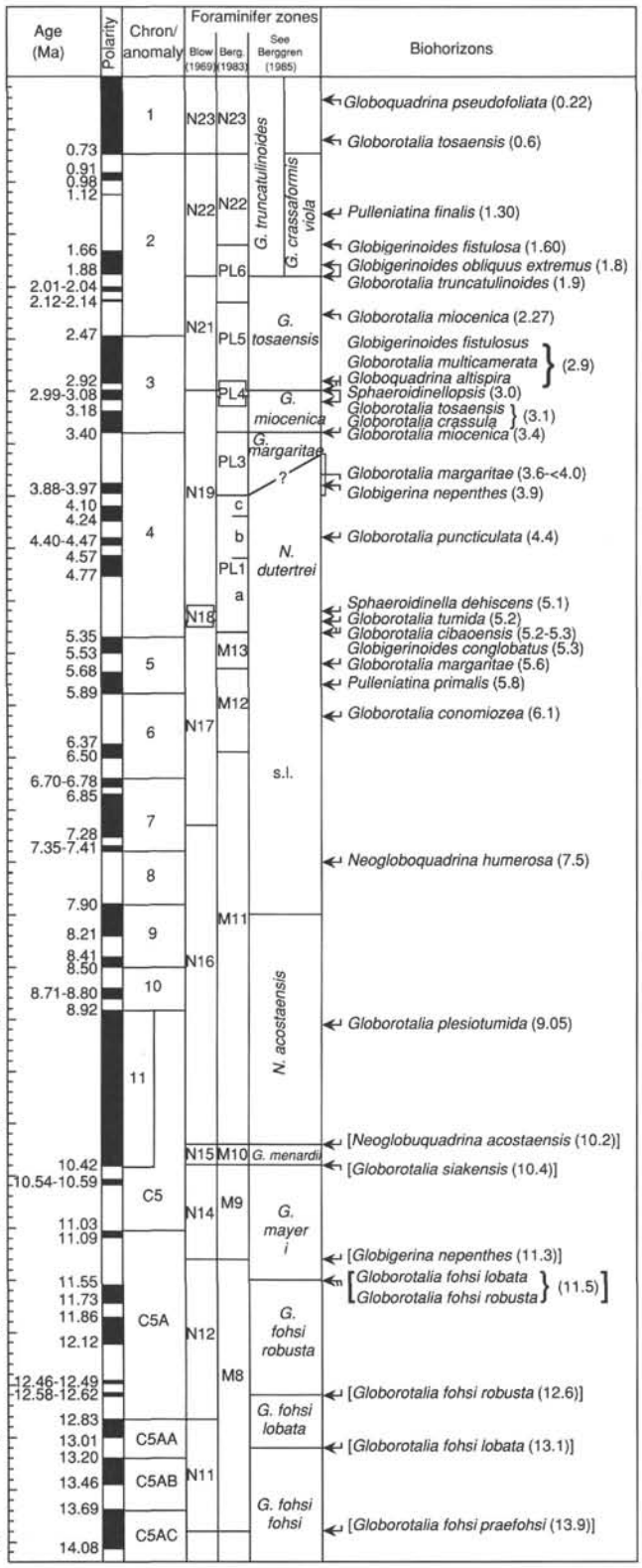

Figure 10. Foraminiferal ages determined by cross-correlating with the GPTS correlation charts assembled for planktonic foraminifers.

Foraminiferal age determinations were cross-correlated using the GPTS correlation charts assembled for calcareous nannofossils (Fig. 9) and for planktonic foraminifers (Fig. 10). In the absence of calcareous nannofossils in Miocene shallow-water carbonates, the middle/late Miocene boundary was identified by either the latest occurrence of the larger benthic foraminifers *Nephrolepidina howchini* or *N. martini* or, when present, the latest occurrence of the planktonic foraminifer *Globorotalia siakensis*.

Smear slides were prepared for each core catcher and for as many samples in between as it was possible to study on board ship. Low sedimentation-rate (condensed zones) or suspected hiatuses were sampled as closely as practical. Standard preparation techniques were used throughout. Slides were examined exclusively with a light microscope, using whatever optical configuration yielded useful results. Most examination was at a magnification of between X1000 and X2000.

Preservation of calcareous nannofossils was recorded as good (G), fair (F), or poor (P). These categories represent subjective impressions having approximately the following meaning:

G (good) = little or no evidence of dissolution and/or overgrowth; diagnostic characteristics are preserved and nearly all specimens (about 95%) can be identified.

F (fair) = dissolution and/or overgrowth are evident; a significant proportion (up to 25%) of the specimens cannot be identified to species with certainty.

P (poor) = severe dissolution, fragmentation, and/or overgrowth has occurred; primary features may have been destroyed, and many specimens cannot be identified at the species level.

Abundances of individual species were estimated for each sample. Six levels of abundance are recorded, with approximate definitions as follows:

W (very abundant): more than 10 specimens per field of view, on average;
A (abundant): 3 to 10 specimens per field of view;
C (common): 1 to 3 specimens per field of view;
F (few): 5 to 15 specimens, total;
R (rare): 2 to 5 specimens, total; and
V (very rare): 1 or 2 specimens, total.

These estimates may have variable accuracy and precision, given that some were made quickly, while others were done more deliberately. Use of these data for subsequent quantitative analyses is not recommended.

Total nannofossil abundances were also estimated and recorded for some sites.

These estimates were recorded as follows:

1. Estimated percentage of coccoliths in the sediment (i.e., the proportion of the sediment consisting of coccoliths). This may be thought of as representing the relative dominance of pelagic sedimentation.
2. Estimated percentage of coccoliths in the carbonate fraction of the sediment.
3. Estimated percentage of the noncarbonate fraction.
4. Estimated percentage of quartz on slide.
5. Estimated percentage of nonquartz siliciclastics on slide.

These last estimates may prove useful for identifying condensed zones, sea-level falls, and so forth, at a later stage of evaluation and interpretation of the paleontological data.

Foraminifers

Sample Preparation

Approximately 10-cm^3 samples were soaked either in plain tap water or in a Calgon solution and washed through a 63-μm sieve with a Calgon solution. Samples that were difficult to disaggregate were treated with a 3% hydrogen peroxide solution. Samples were rinsed with methanol and dried under a heat lamp.

Planktonic Foraminifers

A list of stratigraphically useful species events that were recognized in the Leg 133 material is presented in Figure 10. The zonal scheme given by Blow (1969), with slight modifications by Kennett and Srinivasan (1983), has been employed here. Most ages for the Neogene given by Berggren et al. (1985a) and Barron et al. (1985a, 1985b) were applied. The >125-μm fraction was examined for planktonic foraminifers, and the 63- to 125-μm fraction was studied for the zonal markers if they were absent in the larger size fractions.

The abundance of planktonic foraminifers is defined as follows:

R = rare (<10 specimens),
F = few (10–100 specimens),
C = common (101–500 specimens), and
A = abundant (>500 specimens).

Three classes of foraminiferal preservation were used as follows:

P = poor (almost all specimens were broken and fragments dominated),
M = moderate (30%–90% of specimens exhibited dissolution), and
G = good (>90% of specimens were well preserved and unbroken).

Benthic Foraminifers

The abundance of benthic foraminifers is defined as follows:

R = rare (<10 specimens),
C = common (10–100 specimens), and
A = abundant (>100 specimens).

Three classes of foraminiferal preservation were used:

P = poor (almost all specimens were broken and exhibited dissolution),
M = moderate (30%–90% of specimens exhibited dissolution), and
G = good (>90% of specimens were well preserved and unbroken).

Paleobathymetric Methods

Smaller benthic foraminifers were examined from the >150-mm size fraction. Larger benthic foraminifers either were selected directly from the samples and examined from the >63-mm size fraction or were examined in oriented thin sections. Paleobathymetry estimates using the smaller benthic foraminifers were primarily based on van Morkhoven et al.'s (1986) depth zonations. Bathymetric ranges are as follows: neritic (0–200 m) is divided into inner (0–30 m), middle (30–100 m), and outer (100–200 m); bathyal (200–2000 m) is divided into upper (200–600 m), middle (600–1000 m), and lower (1000–2000 m); and abyssal (>2000 m). The neritic paleobathymetric zonation of Chaproniere (1975) and Carozzi et al. (1976), based on larger benthic foraminifers, was adopted.

PALEOMAGNETISM

Paleomagnetic studies on the *JOIDES Resolution* during Leg 133 included measurement of natural remanent magnetism (NRM), remanence after progressive alternating-field (AF) demagnetization, and magnetic susceptibility. The archive half of the core was subjected to progressive AF demagnetization to remove any weak secondary magnetization and to assess the characteristic (depositional or early post-depositional) remanent magnetization directions for magnetostratigraphic application. Where evidence existed for primary remanence after AF demagnetization, inclination directions were used to assign a magnetic polarity to the sediment column. With the aid of biostratigraphic data, the polarity reversal zones were correlated with the magnetic polarity time scale of Berggren et al. (1985c).

Instruments

The *JOIDES Resolution* maintained two magnetometers for measuring magnetic remanence during Leg 133: a Molspin spinner magnetometer and a 2-G Enterprises (model 760R) pass-through cryogenic superconducting rock magnetometer (SRM). An AF degausser (Model 2G600) capable of alternating fields up to 25 mT is online with the cryogenic magnetometer. Both the SRM and AF coils are encased in a Mu-metal shield, and an automated sample handling system moves the core through the AF coils and magnetometer sense region. The SRM, AF degausser, and sample drive system are controlled by a FASTCOM 4 multiserial communication board in an IBM PC-AT compatible computer. SRM measurements were controlled by a modified version of a University of Rhode Island BASIC program. The magnetometer and ODP orientation conventions are summarized in Figure 11. During Leg 133 operations in the Southern Hemisphere, shipboard inclination values were plotted as positive for normal polarity and as negative for reversed polarity.

The superconducting quantum interference device (SQUID) sensors in the SRM measure magnetization over an interval approximately 20 cm long. The widths of the sensor region suggest that as much as 150 cm^3 of core contributes to the output signal. The large volume of core material within the sensor region allows one to determine remanence accurately for weakly magnetized samples, despite the relatively high background noise related to the motion of the ship. The 2-G SQUID electronics operated at a 1X scale for most sediments recovered during Leg 133.

The output from the cryogenic magnetometer during continuous measurement assumes a uniformly magnetized core and provides reliable directional data when a core section larger than the sensing region is measured. Tests conducted during Leg 133 indicated that in cases where the core is not uniformly magnetized, either through natural processes or artifacts (voids in the core, or differential rotation of segments within the core liner), the values of declination, inclination, and intensity should be treated with caution.

Remanent Magnetization Measurements

Remanence measurements of sediments and rocks were performed by passing continuous, archive-half core sections through the cryogenic magnetometer. NRM measurements were taken at intervals of either 5 or 10 cm along the core and after AF demagnetization at 15 mT. The maximum AF demagnetizing field allowed by ODP policy for archive-half sections

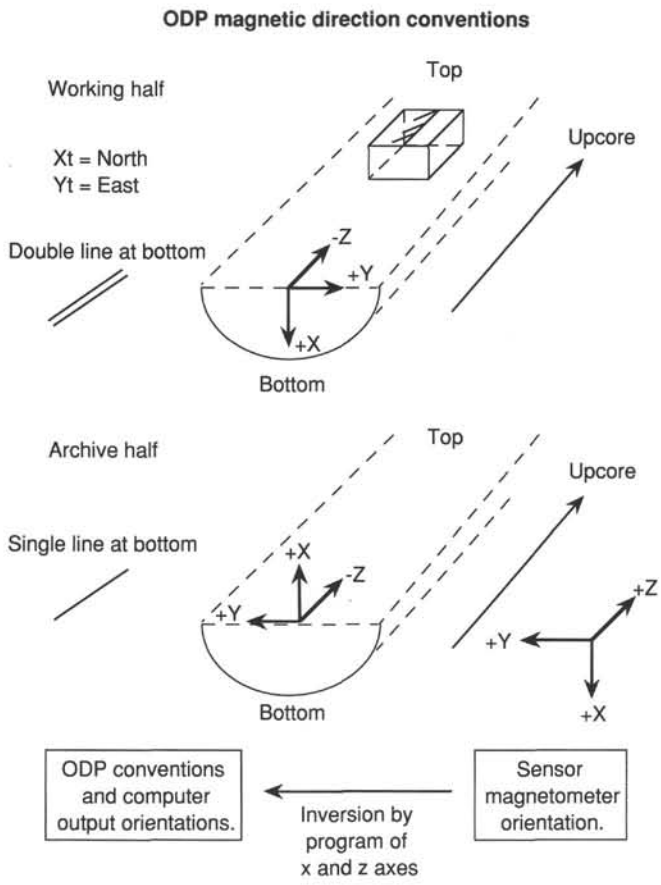

Figure 11. Summary of SQUID sensor and computed orientations of the cryogenic magnetometer program. The shipboard inclination values are plotted as positive for normal polarity and negative for reversed polarity.

is 15 mT or the median destructive field, whichever is lower (assumed to be the 15-mT option).

Discrete samples were taken from APC/XCB sediment cores by pressing an oriented standard plastic sampling box (7 cm^3) into the soft core material. For more consolidated and cemented material, minicores were drilled using a water-cooled nonmagnetic drill bit attached to a standard drill press. The discrete samples collected during Leg 133 were not analyzed on board the ship because of time constraints and relatively weak magnetic moments. Therefore, these samples were saved for analysis in land-based, magnetically shielded laboratories.

Core Orientation

The Multishot core orientation camera, which is capable of recording the azimuthal direction of the double lines on the plastic core liner, was used for many of the APC cores. A summary of oriented cores recovered during Leg 133 is shown in Table 2.

Magnetic Susceptibility Measurements

Whole-core magnetic susceptibilities were measured for all sediment and rock cores using a Bartington Instruments magnetic susceptibility meter (model M.S. 1) having an M.S. 1/CX 80-mm whole-core sensor loop set at 0.47 kHz. The susceptibility meter is part of the MST, which also contains a GRAPE and *P*-wave logger. Magnetic susceptibility of the core sections was measured as part of the physical proper-

Table 2. Summary of HPC core orientation, Leg 133.

Hole no.	Core no.	Inclin. dir. (deg.)	Vertical drift (deg.)	Declin. (0°–360°)
811A	4H	20	0.25	288
	5H	90	0.4	97
	6H	90	0.8	192
	7H	90	0.8	231
	8H	112	0.5	103
	9H	90	1.0	236
	10H	110	0.7	80
	11H	88	0.8	188
	12H	92	0.8	209
	14H	86	1.0	272
	15H	71	0.9	263
	16H	25	0.5	212
	17H	85	1.0	358
	18H	110	1.0	26
	19H	55	0.5	187
	20H	140	0.3	110
	21H	120	0.9	307
	22H	70	0.5	190
	23H	100	0.7	238
811C	3H	25	1.0	280
	4H	70	0.8	42
	5H	20	0.9	176
	6H	40	1.0	231
812A	4H	29	1.3	309
813A	4H	100	1.0	246
	5H	140	1.0	358
	6H	15	0.2	69
	7H	75	0.8	225
	8H	70	0.9	232
	9H	152	2.0	193
	10H	90	0.1	172
	11H	67	0.8	314
	12H	108	0.8	14
	13H	290	0.2	203
	14H	275	0.2	92
	15H	110	0.2	187
	16H	112	0.2	247
	17H	190	0.6	344
	18H	160	0.6	248
	19H	215	0.9	118
	20H	115	0.3	304
	21H	185	1.0	31
813B	4H	120	1.9	4
	5H	140	1.9	39
	6H	145	1.0	207
	7H	125	1.1	289
	8H	150	1.1	132
	9H	160	1.1	60
	10H	125	0.9	162
	11H	165	0.9	89
	17H	67	1.0	288
	18H	35	0.7	198
	19H	60	1.0	265
814A	4H	335	0.5	277
	5H	282	1.6	61
	6H	268	1.0	334
	7H	303	1.0	209
	9H	283	0.9	75
	10H	285	1.0	138
	11H	315	1.0	253
	12H	308	1.0	262
	13H	320	1.0	262
814C	10H	215	1.0	127
	11H	235	1.0	206
	12H	220	0.9	254
	13H	200	1.1	92
815A	6H	55	1.0	37
	7H	62	1.0	82
	8H	40	0.8	86
	14H	50	0.2	136
	15H	30	0.8	227
	16H	85	0.6	106
	17H	90	0.8	106
	18H	45	1.1	294
	24H	47	1.0	209
	25H	60	0.6	136

Table 2 (continued).

Hole no.	Core no.	Inclin. dir. (deg.)	Vertical drift (deg.)	Declin. (0°–360°)
	27H	88	0.6	62
	28H	118	0.7	36
816A	9H	295	1.9	276
	10H	291	2.0	92
	11H	300	2.0	206
817A	4H	145	1.2	322
	5H	220	0.6	46
	6H	145	0.7	314
	7H	125	0.2	301
	8H	155	0.2	140
	9H	—	0	45
	10H	230	0.2	132
	11H	255	0.1	346
	17H	190	0.6	87
	18H	30	0.8	273
	19H	18	0.6	228
	20H	64	0.9	343
	21H	33	0.6	308
817B	4H	274	0.3	96
	5H	156	0.4	328
	6H	—	—	136?
	7H	—	—	136?
	8H	280	0.6	104
	19H	170	0.1	269
	20H	270	0.8	136
	21H	235	0.8	92
	22H	260	0.7	151
818B	4H	170	1.1	357
	5H	171	0.9	76
	6H	145	0.6	229
	7H	160	0.8	40
	8H	225	0.7	134
	9H	115	0.7	282
	10H	165	0.8	205
	11H	105	0.7	200
	12H	180	1.0	128
	13H	195	1.0	152
	19H	170	0.7	261
	20H	180	0.9	201
	21H	172	0.9	314
	22H	185	0.9	355
	23H	182	1.0	127
	24H	210	1.1	46
	25H	205	0.9	245
	26H	213	1.0	337
	27H	202	1.3	72
	28H	225	1.2	103
819A	4H	340	1.0	208
	5H	320	0.8	108
	6H	320	0.3	357
	7H	335	0.9	155
	8H	355	0.8	215
	9H	320	0.9	126
	10H	335	1.0	162
	11H	315	1.0	18
	12H	335	1.0	70
	13H	285	1.1	355
	14H	280	1.2	55
820A	9H	306	1.0	175
	10H	294	1.2	174
	11H	265	1.2	6
	12H	290	1.1	143
	13H	275	1.1	102
	14H	285	1.0	118
	15H	275	0.8	78
820B	4H	155	1.2	171
	5H	177	1.0	98
	6H	155	1.1	168
	12H	142	1.2	5
	13H	135	1.1	358
	14H	145	1.1	35
	15H	138	1.0	235
	16H	160	1.1	350
	17H	160	1.0	341
821A	14H	292	1.0	259
	15H	295	1.0	252
	16H	265	0.9	157

Table 2 (continued).

Hole no.	Core no.	Inclin. dir. (deg.)	Vertical drift (deg.)	Declin. (0°–360°)
821B	4H	90	0.6	173
	5H	85	0.6	132
	6H	95	0.6	217
	7H	92	0.6	82
	8H	80	0.6	345
	9H	90	0.8	62
	10H	65	1.0	204
	12H	106	0.8	17
	13H	65	0.8	196
	14H	75	1.0	6
	15H	66	0.9	161
822A	5H	10	1.6	258
	6H	8	1.5	114
	7H	12	1.5	208
	8H	16	1.2	297
	9H	13	1.0	277
	10H	11	0.8	102
	11H	7	1.2	352
823A	4H	125	1.0	322
	5H	215	0.8	118
	6H	140	0.6	237
	12H	167	0.9	44
	13H	188	0.9	84
823B	4H	226	0.8	57
	5H	52	1.0	325
	6H	18	0.6	84
	7H	37	1.0	214
	8H	10	0.6	357
	9H	68	1.0	247
	10H	8	0.5	28
	11H	30	1.0	208
824A	1H	18	1.0	278
	2H	16	1.3	217
	3H	8	1.0	109
	4H	30	1.0	318
	5H	27	0.9	283
	6H	340	0.8	335
	7H	27	0.5	280
	8H	32	0.8	198
	9H	324	0.8	8

Note: Inclination direction = direction of nonvertical offset.
Vertical drift = variation of drillstem from vertical.
Declination = orientation of double line on liner (working half), ranging from 0°–360°.

ties package (see "Physical Properties" section, this chapter).

Susceptibility is a measure of the ease with which a material can be magnetized. The general trend of the susceptibility data curve was used to characterize the nature of the magnetic material contained within the cored sediment. Susceptibility response is a function of the mineralogy (mainly magnetite) and grain-shape/size of the magnetic minerals within the sediment.

INORGANIC GEOCHEMISTRY

Interstitial Water Chemistry

The shipboard inorganic geochemistry program focused on the retrieval of interstitial waters by means of hydraulic-press-actuated extrusion of samples obtained from whole-round cores. Special attention was given to taking closely spaced samples in the upper 100 m (1 whole-round core sample per core), followed by one sample every third core (length = 5 cm); deeper cores required larger sections for sufficient recovery of interstitial waters. Care was taken that end caps were not sealed with acetone before taking inorganic geochemistry whole-round sam-

Table 3. Analytical methods used during Leg 133.

Analysis	Technique	Reference
Salinity	Goldberg refractometer.	
Alkalinity	Gran titration.	Dyrssen, 1965.
pH	TRIS-BIS buffers.	Bates and Calais, 1981. Bates and Culberson, 1977.
Calcium	EGTA titration.	
Magnesium	EDTA titration	Gieskes and Peretsman, 1986.
Strontium	Absorption spectrometry.	
Potassium	Emmission spectrometry.	
Chlorinity	Mohr titration.	
Ammonia	Colorimetry.	Solorzano, 1969. Gieskes, 1973.
Phosphate	Colorimetry.	Strickland and Parsons, 1968. Gieskes, 1973.
Silica	Colorimetry.	Gieskes, 1973.

Table 4. X-ray calibration.

Sample no.	Mineral (wt %)				Ratio of minerals to calcite		
	CAL.	QUAR.	ARAG.	DOL.	A/C	Q/C	D/C
1	48.92	22.90	19.44	8.74	0.047171	0.061906	0.211701
2	18.86	7.78	65.86	7.49	0.572426	0.05752	0.427832
3	10.50	5.66	78.86	4.98	0.728417	0.14964	0.424101
4	7.11	44.19	43.07	5.63	0.753499	0.858691	0.576072
5	37.02	19.08	8.58	35.32	0.05089	0.097052	0.946885
6	50.62	49.38	0	0	0	0.149829	0.016648
7	51.27	0	48.73	0	0.098542	0.003359	0.009404
8	56.31	0	0	43.69	0.012959	0	0.660187
9	13.55	36.45	50.00	0	0.257724	0.389276	0.028104

Note: CAL. = calcite; QUAR. = quartz; ARAG. = aragonite; DOL. = dolomite; A/C = aragonite/calcite; Q/C = quartz/calcite; D/C = dolomite/calcite.

ples. Additional precautions were taken to minimize the effects of core contamination by drill water through the removal of any suspicious material from the outside of the whole-core sample and along cracks and fissures.

After selection, samples were squeezed using a normal stainless-steel Mannheim-type squeezer at room temperature (Sayles et al., 1973). All samples were filtered through 0.45-mm Gelman acrodisk disposable filters and subsequently subdivided for both shipboard work as well as for future work in shore-based laboratories.

Additional samples were recovered from the WSTP sampler and the wireline packer, whenever these instruments were deployed.

Shipboard analyses performed are listed in Table 3. Procedures for these analyses are summarized, with modifications by Presley (1971), Gieskes (1973, 1974), and Gieskes and Peretsman (1986). The pH was measured on the free H^+ scale using TRIS-BIS buffers (Bates and Calais, 1981; Bates and Culberson, 1977). Alkalinity measurements were calibrated using a 2-mM $NaHCO_3$ solution made in a 0.7-M NaCl solution. As the AA procedures used by ODP have not been generally described and differ slightly from those used previously, we have included a brief description of the methods used during Leg 133.

Strontium

Strontium was measured in the absorption mode at 460.7 nm using an air/acetylene flame. Standards were prepared using stock 1000-ppm Sr solution diluted with a 10,000-ppm La solution. Standards of 1, 3, and 5 ppm were prepared. Samples were diluted using a 10,000-ppm La solution to a dilution of 1:5. This method was found to provide reproducible results to ±3%.

Potassium

Standards were prepared by diluting IAPSO (399.43 ppm K) with distilled water. Solutions were analyzed using the flame emission mode of the Varian AA at a wavelength of 766.5 nm.

Solid Phase Chemistry

Shipboard carbonate carbon and organic carbon/nitrogen analyses were performed on a routine basis using samples provided by the core laboratory as well as for samples collected in the chemistry laboratory.

Total inorganic carbon was determined using a Coulometrics 5011 coulometer equipped with a System 140 carbonate carbon analyzer. Depending on carbonate content, 15 to 70 mg of ground and weighed sediment was reacted in a 2N HCl solution. The liberated CO_2 was titrated in a monoethanolamine solution with a color indicator, while the change in light transmittance was monitored with a photo-detection cell.

X-Ray Diffraction

During Leg 133, quantitative X-ray diffraction analyses were performed to determine relative percentages of aragonite, calcite, quartz, and dolomite. A Philips instrument was calibrated using a series of nine standards. The ratio of the areas of the peaks of interest was obtained relative to calcite and calibrated relative to the same ratio in the standard. The concentration of calcite was calculated assuming that the sample was composed completely of these four minerals. Calibration lines calculated for this method generally agreed within ±5% and are shown in Table 4 and Figures 12 to 14.

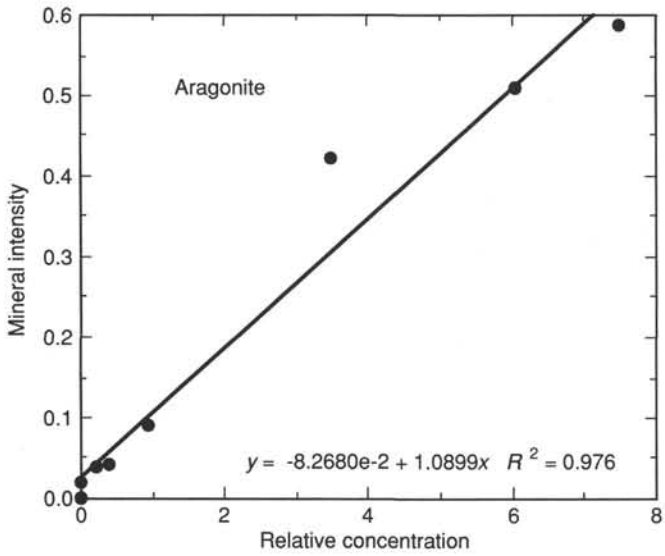

Figure 12. Calibration line for aragonite X-ray diffraction data.

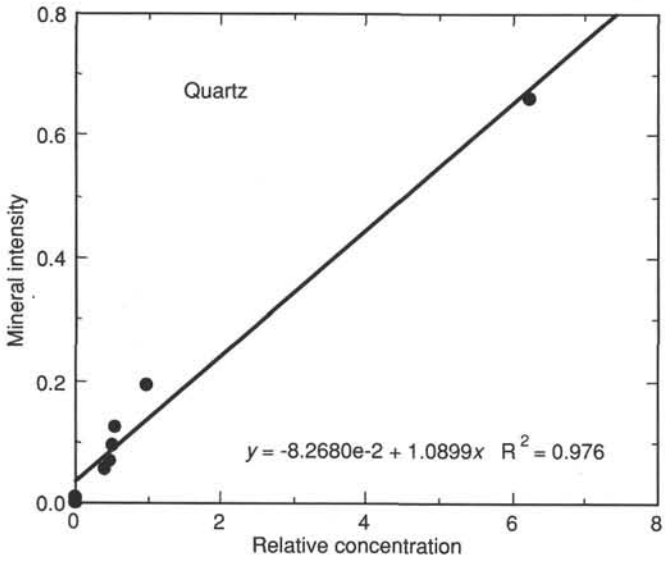

Figure 13. Calibration line for quartz X-ray diffraction data.

Wireline Packer

During Leg 133, a new wireline packer was tested in the sediments. This packer, operated in a logging-tool (wireline) mode, is designed to obtain fluids from the formation *in situ*. The use of this tool is of particular importance when the recovered sediments are cemented and thus are not amenable to normal squeezing methods. Fluids are sampled in a sample bottle sequence, and their chemistry is monitored in the tool to assure quality control.

ORGANIC GEOCHEMISTRY

During Leg 133, shipboard organic geochemistry was conducted to supply a real-time monitoring of volatile hydrocarbons for safety considerations and for an initial characterization of the content and type of gases and sedimentary organic matter. These analyses provide a basis for preliminary site summaries and background for the more-detailed, shore-based studies.

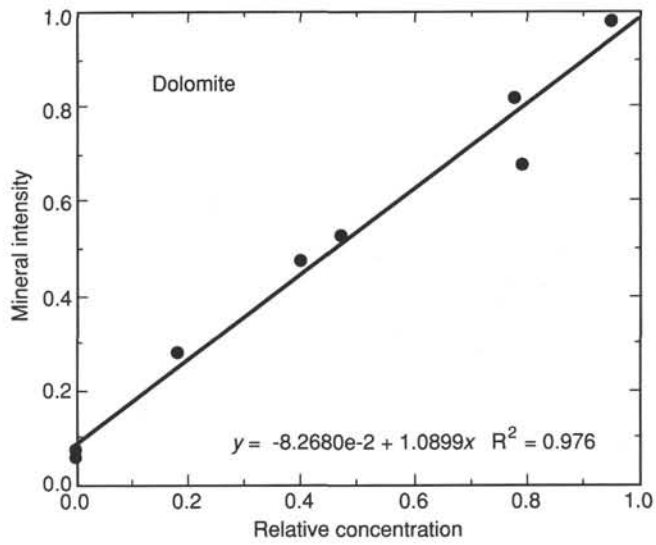

Figure 14. Calibration line for dolomite X-ray diffraction data.

Gas Analyses

As required by safety considerations, the concentrations of the hydrocarbons methane (C_1), ethane (C_2), and propane (C_3) were monitored in the sediment cores at intervals of approximately 10 m.

Gases were extracted from bulk sediments using headspace sampling techniques (Emeis and Kvenvolden, 1986). A 5-cm^3 plug of sediment was taken with a No. 4 cork borer as the core arrived on deck. This sample was placed immediately in a glass vial that subsequently was sealed with a septum and metal crimp and then heated to 70°C and kept at this temperature for 45 min. Gas concentrations have not been normalized to the quantity of sediment in the glass vial.

Gas pocket samples were obtained by expanding gases from visual pockets into pre-evacuated and sealed glass tubes (vacutainers). For this purpose, one end of an injection needle is inserted through the rubber stopper of the vacutainer, with the other end through the plastic liner into the gas pocket.

All headspace gas and vacutainer samples were expanded into a gas-tight syringe and injected into the following:

1. A Hach-Carle AGC Series 100 Model 211 gas chromatograph equipped with a flame ionization detector and a 6-ft × 1/8-in. steel column packed with Porapak N:Q (80%/20%);
2. An HP 5890A NGA gas chromatograph for FID and TCD analyses. The gas chromatographic system employs a 6-ft × 1/8-in. steel column packed with Poropak T, a 3-ft × 1/8-in. steel column with a 13X molecular sieve, a 6-ft × 1/8-in. steel column packed with 80/100 mesh Hayesep R(AW), and a DB1 (1 mm film thickness, J&W). Appropriate automatic valve switching, controlled by an HP 3392 Integrator that also recorded and integrated the count rates, provided a rapid determination of oxygen, nitrogen, carbon dioxide, and hydrocarbons from methane to hexanes. The separation on the FID line was conducted isothermally at 40°C at a flow rate of 2.24 mL/min. Helium was used as carrier gas.

All gas concentrations are reported in parts per million.

Elemental Analyses

Sediments were analyzed on board the ship for inorganic carbon and for total nitrogen, carbon, and sulfur. The total organic carbon (TOC) content of the sediments was then

calculated by subtraction of the inorganic carbon content from the total carbon content. The analyses were performed on sediment residues from headspace gas analyses, while the sediments were freeze-dried prior to analysis.

Total nitrogen, carbon, and sulfur contents were determined using an NA 1500 Carlo Erba NCS analyzer. Bulk samples were combusted at 1000°C in an oxygen atmosphere with addition of vanadium pentoxide, converting organic and inorganic carbon into CO_2 and sulfur to SO_2. These gases along with nitrogen were then separated by gas chromatography and measured with a thermal conductivity detector (TCD). The concentration of organic carbon was then calculated by subtracting the inorganic carbonate component.

Rock-Eval Analyses

The bulk geochemical character of sedimentary organic matter was determined using the Rock-Eval-II pyrolysis technique outlined by Espitalié et al. (1985a, 1985b, 1986). This technique permits a rapid identification of type and maturity of organic matter in ground rock samples of about 100 mg. The pyrolysis technique involves a microprocessor-controlled temperature program that causes the release of hydrocarbons and CO_2 in a stream of helium. The amount of hydrocarbons is determined by a flame ionization detector (FID), whereas for CO_2, the TCD method is employed. Four parameters characterizing organic matter were determined:

1. S_1: Hydrocarbons (mg hydrocarbons per g of rock) that were formed during maturation of organic matter and/or that migrated into the sediments are recorded at pyrolysis temperatures below 300°C.
2. S_2: Corresponds to the release of hydrocarbons generated through thermal cracking of the kerogen matrix as the sediment is heated at 25°C/min from 300° to 550°C during pyrolysis (cycle 1). S_2 also shows the quantity of hydrocarbons that might be produced in this rock, should burial and maturation continue.
3. S_3: The quantity of CO_2 (mg CO_2 per g of rock) produced from pyrolysis of the organic matter at temperatures between 300° and 390°C is detected by the TCD and recorded during cooling.
4. T_{max}: Maturity of the organic material assessed by the temperature at which a maximum release of hydrocarbons from cracking of kerogen during pyrolysis occurs (peak of S_2). The Rock-Eval pyrolyzer also provides information about the type of organic matter through the Hydrogen Index (HI;100 × S_2)/TOC)), Oxygen Index (OI;100 × S_3)/TOC)), and the S_2/S_3 ratio.

Rock-Eval pyrolysis was conducted only on sediment samples containing more than 1% TOC to ensure that no sorption effect influences the geochemical values.

PHYSICAL PROPERTIES

Shipboard determinations of physical properties are the basis for geotechnical stratigraphy studies and provide an important link among the geophysical site survey data, downhole logging results, and the geologic record obtained by coring. Cores are generally sampled with sufficient density to encompass the range of lithologic units recovered from each hole. The properties determined include undrained shear strength, electrical resistivity, compressional wave velocity, bulk density, grain density, porosity, water content, and thermal conductivity. In all discrete measurements used to determine physical properties, we tried to analyze only undisturbed sediment and rock. Boyce (1976) described in detail the techniques employed for determining index properties and compressional wave velocity. Boyce (1977) and Lee (1984) discussed the determination of undrained shear strength. The techniques of both Von Herzen and Maxwell (1959) and Vacquier (1985) were used to determine shipboard thermal conductivities.

Undrained shear strength of the sediment, as described by Boyce (1977) and Lee (1984), was determined using a Wykeham-Farrance motorized vane apparatus with a four-bladed vane that is 1.28 cm long and has a diameter of 1.28 cm. The vane was inserted into the split core section perpendicular to its face (perpendicular to the core axis), to a point where the top of the blade was covered by 4 to 6 mm of sediment. The vane was then rotated at a rate of about 90°/min. until the sediment failed. The undrained shear strength was calculated from the peak torque obtained at failure. Vane testing was stopped when radial cracking or other noncylindrical failure surfaces developed around the vane. Noncylindrical failures were observed in stiffer sediments, which had undrained shear strengths that exceeded approximately 50 kPa. All shear strengths were reported in units of kPa.

Electrical Resistivity and Formation Factor

The electrical resistivity of the sediments was measured every 75 cm using a four-electrode (Wenner) configuration. The electrodes are made of 2-mm-diameter, stainless-steel rods with electrodes, and the difference in potential between the two inner electrodes was measured. The size of the current (typically 50 Ma) was measured over a resistor in the outer circuit. For an infinite and homogeneous medium, resistivity in ohm-meters is given by Equation 1 (Jakosky, 1940):

$$R = K \cdot V/I, \quad (1)$$

where R is the specific resistivity, K is the cell constant, V is the potential difference between the inner electrodes, and I is the current. The primary objective of measuring the resistivity is to determine the formation factor,

$$FF = R/R', \quad (2)$$

where R′ is the resistivity of the pore fluid. We assume that the pore fluid is not substantially different from seawater of normal 3.5% salinity. The resistivity of a seawater standard held in a core liner was measured before and after measuring each core. The formation factor was then computed as the resistivity of the sediment relative to the seawater standard. Uncertainty introduced by assuming that resistivity of the pore water is the same as that of a seawater standard solution is small.

Electrical Resistivity Imaging of Core Samples

We conducted special resistivity experiments for Leg 133 cores. These were prototype experiments that are part of a program to develop a fine-scale resistivity device for imaging cores analogous to the Schlumberger formation microscanner used in logging. Because of the unique nature of this experiment, we have explained it in some detail here. The following discussion of the experiment is taken from Jackson et al. (1990).

High-resolution electrical resistivity measurement techniques for whole-round and split cores are being developed to produce images of electrical and petrophysical properties having sufficient resolution to complement the Schlumberger FMS downhole resistance images. Downhole FMS images presently provide the highest available resolution for downhole data; this is a qualitative technique that should thus

benefit greatly from complementary laboratory measurements.

Laboratory resistivity imaging of cores should be sensitive to the same fabric and structural details that control the downhole images and thus provide a means of quantitatively converting electrical resistance images into other physical/petrophysical properties.

Background

Laboratory measurements have the traditional role of complementing downhole measurements, with a view to providing a calibration of downhole data in terms of petrophysical properties. Laboratory investigations also can lead to greater understanding of the fundamental relationships between geophysical processes and petrophysics of core samples.

The FMS, which was developed by Schlumberger (Ekstrom, 1986), has set new standards in the acquisition of borehole images. This tool uses multiple single-point resistance measurements to assess fine changes in electrical resistivity at the surface of the borehole wall; many examples have been reported in the literature (e.g., Pezard and Luthi, 1988).

These downhole images represent the highest resolution of currently available technology, with measurements on a vertical spacing of 0.1 in. This is achieved using four rows of 0.2-in.-diameter electrode buttons at a separation of 0.4 in. between the nearest centers, while each of the four rows is offset by 0.1 in. to provide even coverage. Thus, one can feasibly produce high-resolution electrical resistance images of the borehole wall.

FMS images may show fine bedding in sedimentary sequences, fractures, foliation, and property contrasts for comparison with visual inspection of the core. These images have immense potential for understanding geological processes and for assessing qualitative petrophysical changes. Resistance measurements are essentially relative and cannot be converted to resistivities with confidence. Furthermore, each button is compensated by equalization techniques to remove stripes from the data. This type of processing permits superb images to be produced, but highlights the point that the technique is a relatively nonquantitative one. Contrasts can be identified, but for example, the resistivity of a sealed fracture cannot be assessed with enough confidence to predict its porosity. Thus, the need to convert downhole FMS images to quantitative resistivities is of considerable importance.

Laboratory resistivity data at a comparable resolution might allow us to interpret FMS images in terms of geological conditions: for example, foliation and fractures might be separated, and anisotropy could be assessed, in addition to enhanced fracture analysis, where porosity and permeability might be predicted at a scale commensurate with the fractures.

Electrical Resistivity Measurements

Laboratory investigations of electrical resistivity require relatively simple measurements, which have been done for many decades. However, this simplicity introduces problems in that no universally accepted common method still does not exist. Electrical conductivities of fluids normally are measured using high-frequency, two-electrode methods for geochemical and hydrogeological investigations, whereas geophysicists favor four-electrode methods, which have been shown as inherently more accurate (Rust, 1952; Brace et al., 1965; Niininen and Kelha, 1979).

The objective has normally been to obtain an average value of the gross resistivity of core samples and plugs. This has the disadvantage of ignoring the smaller-scale features and can be degraded by electrode effects (Jackson et al., 1978). Furthermore, great confusion often exists during assessment of electrode effects and equi-potential surfaces. This results from the complex nature of the electrolyte/ionic and metal/electron interfaces, where an electrochemical barrier to current flow exists. This effect was documented by Guptasarma (1983), who identified problems when assuming Ohm's law during tank modeling experiments using metallic conductors. Here, the electrochemical component of the impedance to current flow was shown as dependent on the magnitude of the current passed.

Core Imaging

Core imaging has been researched using hybrid electrode arrays over the last decade or so, without real impact on petrophysics (Lytle et al., 1977; Lytle and Dines, 1979). These methods tend to use hybrid electrode arrays that often combine the two- and four-electrode resistance measuring methods. As already mentioned, the two-electrode methods suffer from variable electrochemical effects that can degrade large-area electrodes, such as some of the so-called "guard" electrodes that are designed to control where the electric current flows. By comparison, the approach we have adopted is to apply computer-controlled geophysical mapping techniques that have been developed for imaging geological structure (Jackson et al., 1990; Jackson and McCann, 1989; Jackson and Ogilvy, 1990).

This technique involves low-frequency, four-electrode resistance measurements, where all electrodes are taken as points as far as is possible. Thus, the locations in space from which current emanates and the potentials are measured precisely, in contrast to large-area, two-electrode methods. The method we adopted is a substantial development of the linear rectangle or two-dimension gradient array (Kunetz, 1966). This array has many advantages for mapping geological structures, based on high resolution and simple responses that are a direct indication of the underlying resistivity structure.

The potential difference measurements are performed through a pad of 64 stainless steel electrodes spaced on a 4- × 16-electrode grid having a spacing of 0.2 in. Each of the multiple current sources is individually fixed using a control system that permits a uniform current field to be generated using point electrodes. The potential differences are measured on the surface of the core, which may be split if desired. Resolution is limited only by the number of electrode positions. This can be improved by increasing the number of electrodes or repeated offset measurements. The use of point electrodes for both potential and current allows one to control the current field and permits high-resolution potential measurements that do not disturb the flow of current.

The technique is novel in that precise independent control of the current flow is possible and that voltage measurements are not degraded by surface impedances and electrochemical effects. The computer-controlled scanning system was developed specifically for core measurements, but it draws heavily on experience gained during the development of geophysical mapping techniques for geological structures (Jackson and McCann, 1989; Jackson and Ogilvy, 1990). Investigations of electrical anisotropy are possible by defining different directions of current flow using simulated line sources (e.g., Lytle and Dines, 1979) and using constant-current point sources to spatially control the injection of current in the region of interest in a way that is not possible with a single metallic conductor.

Compressional Wave Velocity

Compressional wave velocity measurements were taken for discrete samples that were sufficiently competent to pro-

vide adequate signal strength. Velocities were calculated by determining traveltime of a 500-kHz compressional wave through a measured thickness of sample, using a Hamilton Frame Velocimeter and Tektronix DC 5010 counter/time system. Samples of soft sediment were taken with a special parallel-sided sampling tool. Sample thicknesses (distance) were measured directly from frame lead screw.

Zero traveltimes for the velocity transducers were estimated by linear regression of traveltime vs. distance for a series of distilled water, seawater, and lucite standards. Filtered seawater was used to improve the acoustic contact between the sample and the transducers. Velocities were not recorded when insufficient or extremely variable signals were obtained.

Thermal Conductivity

Whole-round cores were allowed to equilibrate to room temperature for 2 to 4 hr, following MST measurements and prior to measuring thermal conductivities. Thermal conductivity techniques used have been described by Von Herzen and Maxwell (1959) and Vacquier (1985). All thermal conductivity data are reported in units of W/(m · K). Thermal conductivity was calculated from the increase in temperature of the needle recovered over a period of heating of 6 min. Sampled temperatures from the heating time interval of 60 to 240 s were fitted to the curve using a least-squares approximation as follows:

$$T(t) = F \cdot (q/4Q\,k) \cdot \ln(t) + A + Bt, \qquad (3)$$

where:

k = thermal conductivity,
T = temperature,
t = time since heater on,
q = heat input per unit length per unit time,
A, B = constant of a linear temperature drift, and
F = correction factor determined from the calibration tests made on standards prior to the measurement program.

Reliable measurements require that the temperature drift in the sample at the time of measurement be less than 4×10^{-2} °C/min.

Needle probes that connected to a Thermcon-85 unit were inserted into the sediment through holes drilled into the core liner, and thermal drift was monitored. An additional probe was inserted into a reference material to monitor probe behavior. Once temperature had stabilized, probes were heated, and the coefficient of thermal conductivity was calculated as a function of the change in resistance in the probe about every 20 s over a 6-min interval. Where the sediment was too stiff to permit easy insertion of the probe, holes were drilled into the core material before insertion of the probes. We attempted to insert probes at locations along each core section that appeared to be the least disturbed. However, an annulus of disturbed sediment and drill fluid commonly was present along the inside of the liner, which prevented visual identification of the more intact segments in the core.

Index Properties

Index properties of bulk density, grain density, porosity, water content, and void ratio were determined for samples of sediment and rock (as in Ciesielski, Kristoffersen, et al., 1988). Many index property samples had been previously measured for compressional wave velocity, and this enabled us to correlate directly between velocity and index properties to check for possible trends and consistency of data. Samples were weighed using two calibrated Scientech 202 electronic balances that interfaced with a PRO-350 computer, which compensates for the motion of the ship by taking the average weight of 100 samples. Dry sample weight was determined using the same procedure after oven drying at 110°C for at least 24 hr. Sample volumes were measured using a Quantachrome helium penta pycnometer. A pycnometer is not accurate for wet volumes because of helium absorption by water. Therefore, wet volumes also were calculated from dry volumes and weight as follows:

$$\text{Wet Volume} = \text{Dry Volume} + (\text{Wet Weight} - \text{Dry Weight})\,(0.965 \cdot 1.0245), \qquad (4)$$

where 0.965 is the salt factor to correct for any salt precipitated from the pore water, which was assumed to be standard seawater of 3.5% salinity, and 1.0245 is the density of standard seawater at room temperature.

Definitions and units used for the index properties are as follows:

1. Wet bulk density (g/cm^3) = weight of wet sediment/volume of wet sediments;
2. Grain density (g/cm^3) = weight of dry sediment/volume of dry sediments;
3. Porosity (%) = 100 × volume of seawater/volume of wet sediments;
4. Water content (or dry-water content) (%) = 100 × weight of seawater/weight of dry sediments;
5. Void ratio (dimensionless) = volume of seawater/volume of dry sediments.

All values were corrected for salt content of pore fluid, assuming a seawater salinity of 3.5%.

DOWNHOLE MEASUREMENTS

Tool Strings

Downhole logging directly determines physical and chemical properties of formations adjacent to the borehole. Interpretation of these continuous, *in-situ* measurements can yield a stratigraphic, lithologic, geophysical, and mineralogic characterization of the site. After coring is completed at a hole, a tool string is lowered downhole on a seven-conductor cable, and each of several tools in the tool string continuously monitors some property of the adjacent borehole. Of the dozens of different tool strings commonly used in the petroleum industry, three Schlumberger tool strings were used during Leg 133: the geophysical, geochemical, and FMS combinations. The Lamont-Doherty Geological Observatory (L-DGO) temperature tool was attached to the base of the first two tool strings. The Schlumberger well seismic tool and the L-DGO wireline packer were used at selected sites.

The geophysical combination used during Leg 133 is a digital string that consists of the long-spaced sonic tool (LSS), natural gamma-ray tool (NGT), high-temperature lithodensity tool (HLDT), mechanical caliper tool (MCD), and the phasor induction tool (DIT). This tool combination measures compressional wave velocity and provides indicators of the two variables that most often control velocity: porosity, as indicated by density or resistivity, and clay content, as indicated by the NGT.

The geochemical combination used during Leg 133 consists of the NGT, aluminum clay tool (ACT), and gamma-ray spectrometry tool (GST). This tool combination measures the relative concentrations of 12 elements: silicon, calcium, aluminum, iron, titanium, sulphur, hydrogen, chlorine, potassium, thorium, uranium, and gadolinium.

The FMS tool string includes not only the FMS, but also a general purpose inclinometer tool (GPIT) that spatially orients the FMS resistivity map of the borehole wall. This tool string also contains the NGT to allow one to correlate depth of the FMS data with other logs.

Logs

A brief description of logging tools that were run during Leg 133 is given next. A detailed description of logging tool principles and applications is provided in Schlumberger (1972), Serra (1984), and Timur and Toksoz (1985).

Electrical Resistivity

The dual induction tool (DIT-E) provides three different measurements of electrical resistivity, each one having a different depth of investigation. Two induction devices (deep and medium resistivity) send high-frequency alternating currents through transmitter coils, creating magnetic fields that induce secondary (Foucault) currents in the formation. These ground-loop currents produce new inductive signals proportional to the conductivity of the formation, which are recorded by the receiving coils. Measured conductivities then are converted to resistivity. A third device (spherically focused resistivity) measures the current necessary to maintain a constant voltage decrease across a fixed interval in the near-borehole region. Vertical resolution is about 2 m for the medium and deep resistivity devices and about 1 m for the focused resistivity.

Water content and salinity are by far the most important factors controlling the electrical resistivity of rocks. To the first order, resistivity responds to the inverse square root of porosity (Archie, 1942). Other factors influencing resistivity include the concentration of hydrous and metallic minerals, vesicularity, and geometry of interconnected pore space.

Sonic Velocity

The LSS tool uses two acoustic transmitters and two receivers to measure the time required for sound waves to travel over source-receiver distances of 2.4, 3.0, and 3.6 m. The raw data are expressed as time required for a sound wave to travel through 1 ft (0.31 m) of formation; these traveltimes are then converted to sonic velocities. First arrivals for the individual source-receiver paths are used to calculate the borehole-compensated compressional wave velocity. Only compressional wave velocity is determined on board the ship; however, waveforms are recorded to determine shear-wave and possibly improved compressional wave velocities post-cruise. The vertical resolution of the tool is 0.61 m. Compressional wave velocity is controlled predominantly by porosity and lithification; decreases in porosity and increases in lithification can cause velocity to increase.

Natural Gamma Rays

The NGT tool measures the natural radioactivity of the formation. Most gamma rays are emitted by the radioactive isotope ^{40}K and by radioactive elements of the U and Th series. The gamma-ray radiation originating in the formation near the borehole wall is measured by a scintillation detector mounted inside the sonde. Analysis is achieved by subdividing the entire incident gamma-ray spectrum into five discrete energy windows. The total counts recorded in each window for a specified depth in the well are processed at the surface to give the abundances of the elements K, U, and Th.

Because radioactive elements usually are most abundant in clay minerals, the gamma-ray curve often is used to estimate the clay or shale content. However, rock matrices do occur for which radioactivity values range from moderate to extremely high as a result of the presence of volcanic ash, potassic feldspar, or other radioactive minerals.

Mechanical Caliper Device

The MCD tool provides a basic two-dimensional caliper log of the borehole by means of a bowspring-mounted measurement system. The hole diameter (HD) log is used to detect washouts or constrictions. Borehole diameter significantly affects many of the other logging measurements, and the hole diameter is important factor in log correction routines. This caliper tool is subject to sticking when formation mud gets into its mechanical parts, resulting in bimodal (completely open or almost completely closed) readings. By contrast, the hole diameter measurement produced by the HLDT tool is much more reliable. Consequently, during Leg 133, the MCD tool was used primarily for providing centralization and associated improved log quality for the sonic log, rather than for measuring hole diameter.

Lithodensity Tool

The HLDT uses a ^{137}Ce gamma-ray source and measures the resulting flux at six fixed distances from its source. Under normal operating conditions, attenuation of gamma rays is caused chiefly by Compton scattering (Dewen, 1983). Formation density is extrapolated from this energy flux by assuming that the atomic weight of most rock-forming elements is approximately twice the atomic number. A photoelectric effect index is also provided. Photoelectric absorption occurs in the energy window below 150 keV and depends on the energy of the incident gamma ray, the atomic cross section, and the nature of the atom. Because this measurement is almost independent of porosity, it can be used directly as an indicator of matrix lithology. The radioactive source and detector array is placed in a tool that is pressed against the borehole wall by a strong spring arm; position of this spring arm indicates hole diameter. Excessive roughness of the hole will cause some drilling fluid to infiltrate between the skid and the formation. As a consequence, density readings can be artificially low. Approximate corrections can be applied by using caliper data. Vertical resolution is about 0.30 m.

Compensated Neutron Porosity

A radioactive source mounted on the CNT sonde emits fast neutrons (4 MeV) into the formation, where they are scattered and slowed by collisions with other nuclei. When the neutrons reach a low energy level (0.025 MeV), they are captured and absorbed by atomic nuclei such as hydrogen, chlorine, silicon, and boron. The scattering cross section is the quantity that describes the rate at which neutrons are slowed. Because the scattering cross section for hydrogen is about 100 times larger than for any other common element in the crust, most energy dissipation is caused by collisions with water molecules. Therefore, a change in the number of neutrons detected at a receiver can be related to porosity. In practice, an array of detectors is used to minimize the effects of the borehole or drilling fluid. Because water is present both in pores and as bound water (e.g., clay minerals), porosities measured in the presence of hydrous minerals are overestimates of true porosity. The vertical resolution of the tool is theoretically about 0.25 m, but low signal-to-noise ratio degrades this potential resolution. This tool was available for use during Leg 133, but was not used routinely.

Gamma-Ray Spectrometry Tool

The GST tool consists of a pulsed source of 14-MeV neutrons and a gamma-ray scintillation detector. A surface computer performs spectral analysis of gamma rays that result

from interactions of neutrons emitted by the source with atomic nuclei in the formation (Hertzog, 1979). Characteristic sets of gamma rays from six elements dominate the spectrum, permitting calculation of six elemental yields: Ca, Si, Fe, Cl, H, and S. As their sum is always one, they do not reflect the actual composition of the elements. Therefore, ratios of these yields are used often for interpreting the lithology, porosity, and salinity of the formation fluid.

Aluminum Clay Tool

Aluminum abundance, as measured by the ACT, is determined by neutron-induced (cf. chemical source) late gamma-ray spectrometry. By placing NaI detectors both above and below the neutron source, contributions from natural gamma-ray activity can be removed. Calibration to weight percent of the elements is performed by taking irradiated core samples of known volume and density and measuring their gamma-ray output while placed in a jig attached to the logging tool (generally after logging).

Formation Microscanner

The FMS produces high-resolution microresistivity images or structural maps of the borehole wall that can be used for interpreting sedimentological or structural details and for determining orientations of fractures and breakouts. The FMS is a new tool that was first deployed during Leg 126; it has largely replaced the acoustic televiewer for these purposes. It consists of 16 electrode "buttons" on each of four orthogonal pads that are pressed against the borehole wall. These electrodes are 5 mm in diameter and are arranged in two diagonally offset rows of eight electrodes each, producing a maximum resolving width of 2.5 mm.

Each pad is attached to a movable arm for maintaining pad contact against the borehole wall, and each pair of opposing arms gives a caliper measurement. The maximum opening for each opposing pair is 37 cm (14.5 in.); in larger holes, usually only two of the four pads contact the borehole wall and obtain useful data.

The raw data undergo extensive processing to transform the individual microresistivity traces into complete, spatially-oriented images. Because of shipboard capabilities for processing during Leg 133, only limited reprocessing was possible at sea. All FMS data were processed post-cruise, and final processed images are included on microfiche in this volume. During Leg 133 FMS logging, two passes were always run through the openhole interval; only one pass is presented on the microfiche.

Applications of the FMS images include: (1) detailed correlating of coring and logging depths; (2) orientating of cores; (3) mapping of fractures, faults, foliations, and formation structures, and (4) determining strikes and dips of bedding. The FMS also can be used to measure stress in the borehole through breakout delineation. In an isotropic, linearly elastic rock that has been subjected to an anisotropic stress field, breakouts form in the direction of the least principal horizontal stress.

General Purpose Inclinometer Tool

This tool provides a measurement of borehole inclination, the orientation of the tool with respect to Earth's magnetic field using a three-component magnetometer, and tool motion using an accelerometer. The GPIT is run with the FMS to provide spatial orientation of borehole wall images.

Vertical Seismic Profile–Well Seismic Tool (WST)

A vertical seismic profile (VSP) experiment was included during Leg 133 to determine the detailed velocity-depth structure of the drilled section and to provide an accurate correlation between the drilled section and the site-survey seismic reflection data. VSP measurements not only provide such seismic information for the interfaces penetrated by the borehole, but also permit delineation of reflecting interfaces below the bottom of the borehole (Gal'perin, 1974).

The seismic source for the VSP is a single 1.5-L (80-in.^{3}) water gun suspended from a buoy at a water depth of about 10 m; this source is the same water gun used during the seismic survey when approaching the site. Signals are received by the Schlumberger WST, which is clamped in the hole, and are recorded with the Schlumberger logging computer. The depth interval between clampings can vary; during Leg 133, it averaged about 25 m. Several shots are fired at each level within the borehole to permit stacking of data. Initial shipboard processing is accomplished with Schlumberger Quick-Look software.

Water Sampler, Temperature, Pore Pressure Tool (WSTP)

This tool has a thin, stainless-steel probe that is pushed ahead of the bit into the undisturbed sediments at the bottom of the hole. The WSTP can measure either sediment temperature or pore-fluid pressure, plus collect a pore-water sample at a preset time. When configured to measure temperature, the tool consists of a thermistor mounted at the end of the probe, a self-contained recorder, a timer to open the fluid-sampling valve, and a 16-V power supply. For pore-pressure configuration, the instrument is fitted with a hollow probe tipped with a sintered stone, permitting a hydraulic connection between the end of the probe and an absolute pressure transducer. A second transducer is configured to monitor hydrostatic pressure. Pore fluid is collected through a filter block above the probe (Barnes, 1988).

During operation, the WSTP tool is mounted inside a core barrel and is lowered down the drill pipe by wireline, while the bit is held above the bottom of the hole. The tool is held briefly above the mud line to measure reference values of either temperature or pressure. The WSTP then is lowered and latched into place, with the probe tip extending 1.1 m ahead of the bit. The drill string is lowered, and the probe is forced into the bottom. A collated delivery system allows the probe to retract back up inside the bit should the formation prove too hard for penetration. With an APC/XCB bottom-hole assembly, the bit can be decoupled from the tool after penetration, so that the probe will not be disturbed by drill-string heave.

Penetration of about 70 cm is required within about 3 hr of drilling so that the temperature of the formation is undisturbed by the effects of cold circulation fluid. The thermistor/recording package has a nominal resolution of about 10 ohms, or 0.01° at 25°C. The relatively short length of the narrow probe appears to permit only a few minutes of undisturbed measurements before a thermal disturbance is conducted down from the larger-diameter section above. This limits the accuracy of temperature extrapolations to about 0.1° to 0.2°C. The pressure transducers have resolution of about 8 to 10 psi. Significant disturbance of the formation results from insertion of the probe, but because the instrument cannot be left in position to permit this disturbance to decay completely, extrapolation to equilibrium is required. The theory of measurement is presented in Erickson et al. (1975). A review of thermal data obtained with this type of probe during the DSDP program is given in Hyndman et al. (1987).

Temperature Tool

The L-DGO temperature tool is a self-contained tool that can be attached to any Schlumberger tool string. Data from two thermistors and a pressure transducer are collected every

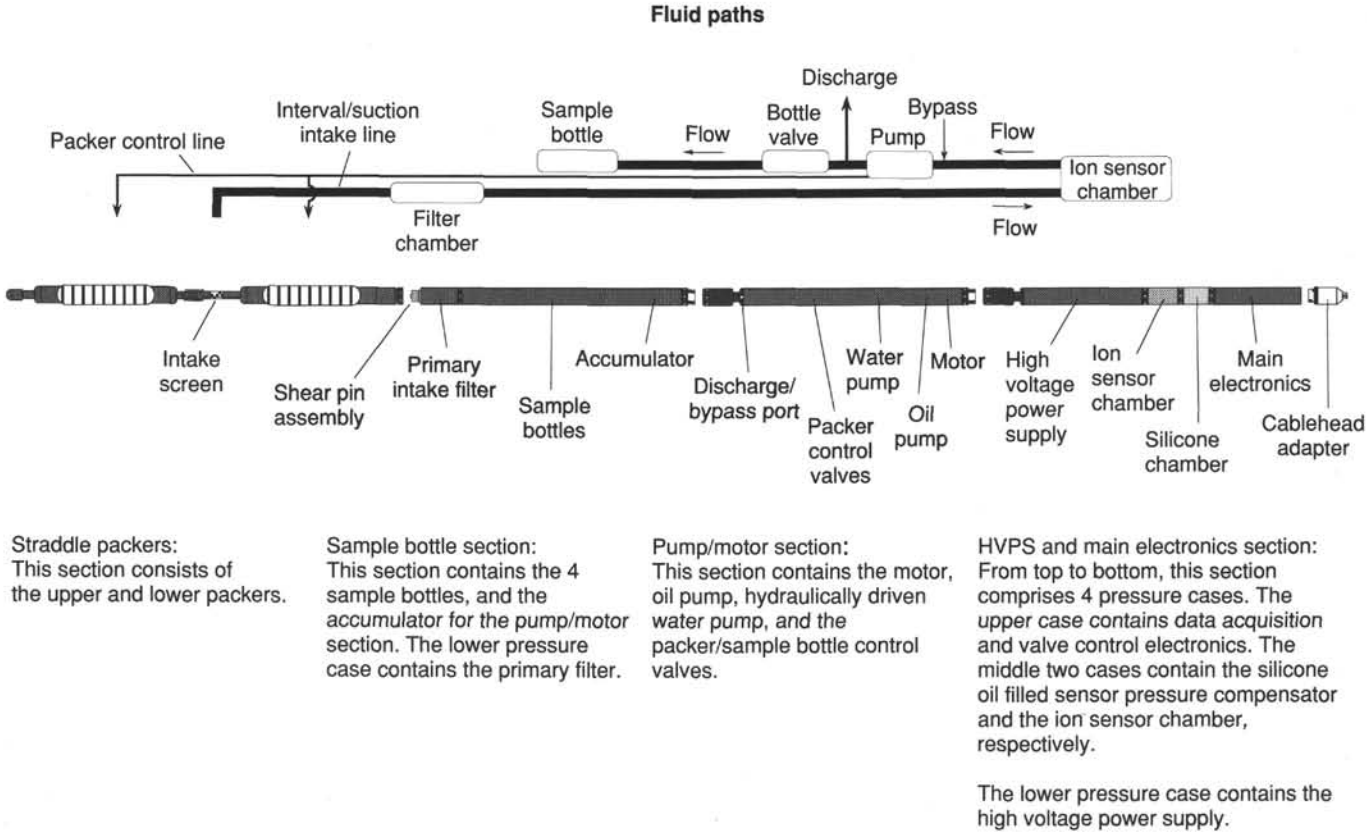

Figure 15. Overview of wireline packer tool design, showing fluid flow paths and configuration of basic components of the wireline packer. The sonde is approximately 45 ft long overall; fluid path from interval to bottle is approximately 55 ft.

0.5 to 5.0 s and then stored in a Tattletale computer within the tool. Following the logging run, data are downloaded from the Tattletale to the Masscomp computer for analysis. A fast-response thermistor (although low in accuracy) can detect sudden, very small temperature excursions caused by fluid flow from the formation. A slow-response thermistor has high accuracy and can be used to estimate heat flow, if one knows the history of drilling-fluid circulation in the hole and if one has at least two temperature logs (Jaeger, 1961). Data are recorded as a function of time; conversion to depth can be based on the pressure transducer or, preferably, on simultaneous recording by Schlumberger of both depth and time.

Wireline Packer

The wireline packer (Fig. 15), designed and built by TAM International, is a discrete-zone, pore-fluid sampler. Except for tool testing, Leg 133 was the first time that this tool has ever been used; consequently, a detailed description of the tool, including figures, is included here. The tool is run via a standard seven-conductor logging cable. Unlike a drill-string packer, which is actuated by dropping a go-devil and pumping through the pipe, the wireline packer is controlled by a surface computer in either the winch room or the Downhole Measurements Laboratory. No hydraulic connection with the surface is required, because the tool contains an electrically operated downhole pumping system. The wireline packer is a straddle tool, meaning that it has two distinct inflation elements. When inflated, the elements isolate a vertical zone approximately 1 m long from which fluid is extracted. Because it must pass through the drill pipe and the bottom-hole assembly, the outer diameter of the packer is limited by the 3.80-in. inner diameter of standard ODP bottom-hole assemblies. The two packer elements will inflate to a maximum of 12 in. at a pressure of about 350 psi differential. Differential pressure is kept relatively low to prevent rupturing of the bladders in the packer elements, which are strained by high expansion.

Following packer inflation, fluid is drawn from the interval isolated by the packer elements and pumped out to the annulus. The pump has an output of approximately 1 gal/min and a maximum drawdown of about 350 psi. Actual pump rates and zone pressures are controlled by the permeability of the formation. Zone and packer pressures, temperature, and fluid chemistry (concentrations of sodium, calcium and pH) are monitored and digitally transmitted to the surface continuously.

By monitoring the geochemical data in real time, the operator can determine when a reasonable concentration of "virgin" formation fluid is present in the system and can redirect fluid flow into one of four sampling bottles. These sampling bottles are similar in design to a syringe, with each having a capacity of about 400 mL. Each bottle is equipped with a check valve to maintain fluid pressure following sampling. Once a sample has been collected, the packers can be deflated and the tool moved to a new location. At the completion of the sampling program, the tool is drawn back up inside the bit and returned to the surface, where the samples are removed for analysis.

Quality of Log Data

The quality of log data may be seriously degraded in excessively large sections of the borehole or by rapid changes in the hole diameter. Resistivity and velocity measurements are less sensitive to borehole effects, whereas the nuclear measurements (density, neutron porosity, and both natural

and induced spectral gamma ray) are most seriously impaired, because of the large attenuation by the borehole fluid. If a hole-size (caliper) log is obtained, corrections can be applied to the various logs to reduce the effects of hole-size variations and, generally, any departure from the conditions under which the tool was calibrated.

Different logs may have small mismatches in depths caused by either cable stretch or ship heave during recording. Small errors in depth-matching can impair the results in zones of rapidly varying lithology. To minimize such errors, a hydraulic heave compensator adjusts for rig motion in real time. Precise depth-matching of logs with cores cannot be obtained in zones where core recovery is low because of the inherent ambiguity of placing the recovered section within the interval cored.

Analysis of Logs

During logging, incoming data were observed in real time on a monitor oscilloscope and simultaneously recorded on digital tape in the Schlumberger logging unit. After logging, the Schlumberger tape was read by the Masscomp computer system in the Downhole Measurements Laboratory and reformatted to a file format compatible with the Terralog log-interpretation software package. Rather than being a "black box," Terralog is an interactive system consisting of many log manipulation and plot options. Thus, log analysis and interpretation varied in duration and procedure for each site. Virtually all of the log interpretation reported here was conducted aboard the ship; minor additional analyses and interpretations were undertaken after the cruise, using a companion system at L-DGO's Borehole Research Laboratory.

Reprocessing of Logs

Raw GST logs for Leg 133 are shown following the barrel sheets for each site at which the GST was run. Raw count rates for six elements (Ca, Si, Fe, S, Cl, and H) were obtained in real time by the Schlumberger data acquisition software. Post-cruise reprocessing, using a Schlumberger Elite 1000 workstation and proprietary Schlumberger software, used a revised algorithm to invert the gamma-ray spectrum at each depth for titanium, gadolinium, and potassium, in addition to the six elements (Ca, Si, Fe, S, Cl, and H) in the shipboard inversion. Although Gd is present in concentrations of only a few parts per million, its neutron-capture cross section is so large that it can account for 10% to 30% of the total gamma-ray spectrum. Inclusion of these additional elements improves the quality of the overall inversion, in particular the accuracy of calculated abundances of Ca, by converting sources of unaccounted variance to signals. However, the determined K concentrations are less accurate than those from the NGT, and the H concentrations are less accurate than those from the neutron tool.

When both the geophysical and geochemical Schlumberger tool strings are run, further reprocessing of geochemical logs is possible. The relative abundances of Ca, Si, Fe, Ti, Al, K, S, Th, U, and Gd are used to calculate a log of predicted photoelectric effect. The difference between this log and the actual photoelectric effect log can be attributed to the only two major elements not directly measured: magnesium and sodium. Major elements are converted from volume percent to weight percent using logs of total porosity (bound water plus pore water) and density. Major elements are expressed in terms of oxide dry weight percent, based on the assumption that oxygen is 50% of the total dry weight.

If GST data are available, but not enough log types have been run to permit complete solution for oxide weight percentage, another processing step is performed. Omitting Cl and H, the yields of the other GST elements (Ca, Si, Fe, Ti, S, K, and Gd) are totaled, and each is expressed as a fraction of this total yield. This procedure corrects for porosity and variations in count rate. Although the absolute abundance of each element is not determined, downhole variations in relative abundance are indicated.

All geochemical logs discussed or shown in this volume are raw logs obtained on board the ship. Results of post-cruise reprocessing of these data will be presented as a data report in the Leg 133 *Scientific Results* volume.

Sonic logs obtained in real time are not based on complete waveform analysis, but on a thresholding technique that attempts to detect the compressional wave arrival by a first-break criterion. Occasionally, this technique fails and either the threshold is exceeded by noise or the first compressional arrival is below the threshold. This phenomenon, called cycle skipping, creates spurious spikes on the sonic log. For every site logged site during Leg 133, raw traveltimes were reprocessed with an algorithm designed to reject cycle skipping (Leg 105; Shipboard Scientific Party, 1987). This algorithm also calculates a semiquantitative estimate of variations in hole size.

Synthetic Seismograms

Synthetic seismograms are generated from logging data obtained with the LSS tool. The bulk-density log from the LDT tool, or a pseudodensity log created from other logs, is required in addition to the slowness log. In many cases, a simple constant-density log can be utilized. Experience shows that this often gives surprisingly good results, because both velocity and density are usually controlled by the same parameter: porosity. When velocity and density are highly correlated, synthetic seismograms that use a constant density log or an actual density log are virtually identical.

Slowness and density logs are used in a program that generates an impedance log (velocity × density), which is convolved with a zero-phase Ricker or other assumed wavelet. The frequency of this wavelet can vary, depending on the source that generated the original seismic profile. A 30-Hz wavelet is capable of a vertical resolution on the order of 30 m; thus, reflectors cannot generally be attributed to any small-scale lithologic horizons. The synthetic seismogram is calculated based on a convolutional model having interbed multiples.

To obtain the best possible match between the synthetic seismogram and the site-survey seismic profiles, the source signature of the BMR *Rig Seismic* 80-in.^{3} water gun used for collecting the data should be used during convolution. In the absence of a measured source signature, we tried to reproduce it using a generalized seafloor-reflected arrival derived by examining all the site-survey seismic profiles and selecting "clean" seafloor reflections. These reflections were chosen from areas where little chance exists for interference with the reflections from shallow geological features, and where the reflection had a consistent form over many traces. Selected reflections were then averaged to produce an approximation of the source signature. This analysis was conducted using SEG normal polarity, 24-fold stacked seismic sections that had been processed without deconvolution and that were displayed without AGC and with a 50- to 120-Hz bandpass filter up to 300 ms below the seafloor. Two versions of the source signature were prepared in this manner, and at some sites, the synthetic seismograms computed using these signatures were compared with those computed using Ricker wavelets of different frequencies. One of the seafloor reflection-derived signatures produced synthetic seismograms that

consistently had a good match with the actual seismic data over the site.

At some logged sites, the synthetic seismogram is shown overlying the seismic section, as well as the velocity log in two-way traveltime and the depth below seafloor. Each synthetic seismogram extends for one wavelet length below the lower limit of log data. This 60-ms interval of synthetic seismogram is incomplete and best disregarded because it is only a response to the lowest impedance data, not the usual superposition of wavelet responses to 60 ms of adjacent impedance variations.

REFERENCES

Archie, G. E., 1942. The electrical resistivity log as an aid in determining some reservoir characteristics. *J. Pet. Tech.*, 5:1–8.

Barnes, R. O., 1988. ODP *in-situ* fluid sampling and temperature measurement: a new wireline tool. *In* Mascle, A., Moore, J. C., et al., *Proc. ODP, Init. Repts.*, 110: College Station, TX (Ocean Drilling Program), 55–63.

Barron, J. A., Keller, G., and Dunn, D. A., 1985a. A mulitiple microfossil biochronology for the Miocene. *In* Kennett, J. P. (Ed.), *The Miocene Ocean: Paleoceanography and Biogeography*. Geol. Soc. Am. Mem., 163:21–36.

Barron, J. A., Nigrini, C. A., Pujos, A., Saito, T., Theyer, F., Thomas, E., and Weinreich, N., 1985b. Synthesis of biostratigraphy, central equatorial Pacific, Deep Sea Drilling Project Leg 85: refinement of Oligocene to Quaternary biochronology. *In* Mayer, L., Theyer, F., et al., *Init. Repts. DSDP*, 85: Washington (U.S. Govt. Printing Office), 905–934.

Bates, R. G., and Calais, J. G., 1981. Thermodynamics of the dissociation of Bis. H^+ in seawater from 5° to 40°C. *J. Solution Chem.*, 10:269–279.

Bates, R. G., and Culberson, C. H., 1977. Hydrogen ions and the thermodynamic state of marine systems. *In* Anderson, N. R., and Malahoff, A. (Eds.), *The Fate of Fossil Fuel CO_2 in the Oceans:* New York (Plenum Press), 45–61.

Berggren, W. A., Kent, D. V., and Flynn, J. J., 1985a. Paleogene geochronology and chronostratigraphy. *In* Snelling, N. J. (Ed.), *Geochronology and the Geologic Time Scale*. Geol. Soc. London Mem., 10:141–195.

Berggren, W. A., Kent, D. V., and Van Couvering, J. A., 1985b. Neogene geochronology and chronostratigraphy. *In* Snelling, N. J. (Ed.), *Geochronology and the Geologic Time Scale*. Geol. Soc. London Mem., 10:211–260.

Berggren, W. A., Kent, D. V., Flynn, J. J., and Van Couvering, J. A., 1985c. Cenozoic Geochronology. *Geol. Soc. Am. Bull.*, 96:1407–1418.

Blow, W. H., 1969. Late middle Eocene to Recent planktonic foraminiferal biostratigraphy. *Proc. 1st Int. Conf. Planktonic Microfossils*, 1:199–422.

Boyce, R. E., 1976. Definitions and laboratory techniques of compressional sound velocity parameters and wet-water content, wet-bulk density, and porosity parameters by gravimetric and gamma ray attenuation techniques. *In* Schlanger, S. O., Jackson, E. D., et al., *Init. Repts. DSDP*, 33: Washington (U.S. Govt. Printing Office), 931–958.

_____, 1977. Deep Sea Drilling Project procedures for shear strength measurement of clayey sediment using modified Wykeham-Farrance laboratory vane apparatus. *In* Barker, P. E., Dalziel, I.W.D., et al., *Init. Repts. DSDP*, 36: Washington (U.S. Govt. Printing Office), 1059–1068.

Brace, W. F., Orange, A. S. and Madden, T. R., 1965. The effect of pressure on the electrical resistivity of water saturated crystalline rocks. *J. Geophys. Res.*, 70:5669–5678.

Carozzi, A. V., Reyes, M. V., Ocampo, V. P., 1976. Microfacies and microfossils of the Miocene reef carbonates of the Philippines. *Phil. Oil Devel. Comp., Spec. Publ.*, 1:1–79.

Chaproniere, C.G.H., 1975. Paleoecology of Oligocene-Miocene larger foraminifera. *Alcheringa*, 1:37–58.

_____, 1981. Australasian mid-Tertiary larger foraminiferal associations and their bearing on the East Indian Letter Classification. *J. Austral. Geol. Geophys.*, 6:145–151.

Ciesielski, P. F., Kristoffersen, Y., and Shipboard Scientific Party, 1988. Explanatory Notes. *In* Ciesielski, P. F., Kristoffersen, Y., et al., *Proc. ODP, Init. Repts.*, 114: College Station, TX (Ocean Drilling Program), 3–22.

Dewen, J. T., 1983. *Essentials of Modern Open Hole Log Interpretations*: Tulsa (Penwall).

Dunham, R., 1962. Classification of carbonate rocks according to depositional texture. *In* Ham, W. E. (Ed.), *Classification of Carbonate Rocks*: Tulsa (Am. Assoc. Petrol. Geol.), 108–121.

Ekstrom, M., Dahan, C. A. Chen, M., Lloyd, P. M. and Rossi, D. J., 1986. Formation imaging with microelectrical scanning arrays. *Trans. Soc. Prof. Well Logging Anal.*, Paper BB, Houston.

Embry, A. F., and Klovan, J. E., 1971. A late Denovian reef tract on northeastern Banks Island, Northwest Territories. *Bull. Can. Pet. Geol.*, 19:730–781.

Emeis, K.-C., and Kvenvolden, K. A., 1986. Shipboard organic geochemistry on *JOIDES Resolution*. *ODP Tech. Note No. 7*.

Erickson, A. J., Von Herzen, R. P., Sclater, J. G., Girdler, R. W., Marshall, B. V., and Hyndman, R. D., 1975. Geothermal measurements in deep-sea boreholes. *J. Geophys. Res.*, 80:2515–2528.

Espitalié, J., Deroo, G., and Marquis, F., 1985a. La pyrolyse Rock-Eval et ses applications. *Rev. Inst. Fr. Petr. Eds. Technip, 40-5:563–579*.

_____, 1985b. La pyrolyse Rock-Eval et ses applications. *Rev. Inst. Fr. Petr. Eds. Technip.*, 40-6:755–784.

_____, 1986. La pyrolyse Rock-Eval et ses applications. *Rev. Inst. Fr. Petr. Eds. Technip.*, 41-1:73–89.

Fisher, R. V., and Schmincke, H. U., 1984. *Pyroclastic rocks*: Berlin (Springer-Verlag).

Gal'perin, E. I., 1974. *Vertical Seismic Profiling*. Soc. Explor. Geophys. Spec. Publ., 12.

Gealy, J. M., Winterer, E. L., and Moberly, R., 1971. Methods, conventions and general observations. *In* Winterer, E. L., Riedel, W. R., et al., *Init. Repts. DSDP*, 7(Pt. 1): Washington (U.S. Govt. Printing Office), 9–26.

Gieskes, J. M., 1973. Interstitial water studies, Leg 15–alkalinity, pH, Mg, Ca, Si, PO_4, and NH_4. *In* Heezen, B. C., MacGregor, I. D., et al., *Init. Repts. DSDP*, 20: Washington (U.S. Govt. Printing Office), 813–829.

_____, 1974. Interstitial water studies, Leg 25. *In* Fisher, R. L., Bruce, E. T., et al., *Init. Repts. DSDP*, 25: Washington (U.S. Govt. Printing Office), 361–394.

Gieskes, J. M., and Peretsman, G., 1986. Water chemistry procedures on board the *JOIDES Resolution*–some comments. *ODP Tech. Note*, 5:46.

Guptasarma, D., 1983. Effect of polarisation on resistivity modelling. *Geophysics*, 48(1):98–106.

Hertzog, R., 1979. Laboratory and field evaluation of an inelastic-neutron-scattering and capture gamma ray spectroscopy tool. *Soc. Pet. Eng. Pap.*, 7430.

Hyndman, R. D., Langseth, M. G., and Von Herzen, R. P., 1987. Deep Sea Drilling Project geothermal measurements: a review. *Rev. Geophys.*, 25:1563–1582.

Jackson, P. D., Taylor, S. D., and Stanford, P. N., 1978. Resistivity-porosity-particle shape relationships for marine sands. *Geophysics*, 43(6):1250–1268.

Jackson, P. D., and McCann, D. M., 1989. Electrical resistivity surveying to detect concealed geological structures during site investigations. *Proc. 2nd Int. Conf. on Foundations and Tunnels* (19–21 September): London (Univ. of London).

Jackson, P. D., Lovell, M. A., Pitcher, C., Green, C. A., Evans, C. J., Flint, R. and Forster, A., 1990. Elecrical resistivity imaging of core samples. *Proc. Euro. Core Analysis Symp. (Eurocas I)*: London (So. Core Analysts), May 10–12, 1990.

Jackson, P. D., and Ogilvy, R. D., 1990. Electrical resistivity imaging for the assessment of geological structures in site investigation (remote sensing and geophysical techniques). *Proc. 6th Int. Congr. of Int. Assoc. Eng. Geol.* (Amsterdam), 6–10 August 1990.

Jaeger, J. C., 1961. The effect of the drilling fluid on temperatures measured in boreholes. *J. Geophys. Res.*, 66:563–569.

Jakosky, J. J., 1940. *Exploration Geophysics*: Los Angeles (Times-Mirror Press).

Kennett, J. P. and Srinivasan, M. S., 1983. *Neogene Planktonic Foraminifera*: Stroudsburg, PA (Hutchison Ross).

Kunetz, G., 1966. Principles of direct current resistivity prospecting. *Geoexplor. Monogr. Ser. 1, No. 1*: Berlin (Gerbruder Borntaeger).

Lee, H. J., 1984. State of the art: laboratory determination of strength of marine soils. *In* Chaney, R. C., and Demars, K. R. (Eds.) *Strength Testing on Marine Sediments: Laboratory and In-situ Measurements*. ASTM Spec. Tech. Publ., 883:181–250.

Lytle, R. J., and Dines, K. A., 1979. An impedance camera: a system for determining the spatial variation of electrical conductivity. *Lawr. Liver. Lab. Rept.*, UCRL-52413:1–11.

Lytle, R. J., Duba, A. G., and Willows, J. L., 1977. Surface methods for determining the electrical conductivity of core samples. *Lawr. Liver. Lab. Rept., UCRL-52311:1–21.*

Martini, E., 1971. Standard Tertiary and Quaternary calcareous nannoplankton zonation. *In* Farinacci, A. (Ed.), *Proc. 2nd Planktonic Conf.* (Rome, 1970), 2:739–785.

Matthews, D. J., 1939. *Tables of Velocity of Sound in Pore Water and in Seawater: London (Admiralty, Hydrog. Dept.).*

Mazzullo, J. M., Meyer, A., and Kidd, R., 1987. New sediment classification scheme for the Ocean Drilling Program. *In* Mazzullo, J., and Graham, A. G. (Eds.), *Handbook for Shipboard Sedimentologists*. ODP Tech. Note, 8:45–67.

van Morkhoven, F.P.C.M., Berggren, W. A., Edwards. A. S., et al., 1986. Cenozoic cosmopolitan deep-water benthic foraminifera. *Mem. Cent. Rech. Explor. Prod. Elf Aquitaine, 11.*

Munsell Soil Color Charts, 1971: Baltimore (Munsell Color).

Niininen, H., and Kehla, V., 1979. Construction of a wide-range specific resistivity meter with logarithmic output. *J. Phys. E. Sci. Instrum.*, 12:261–263.

Okada, H., and Bukry, D., 1980. Supplementary modification and introduction of code numbers to the low-latitude coccolith biostratigraphic zonation (Bukry, 1973; 1975). *Mar. Micropaleontol.*, 5(3):321–325.

Pezard, P. A., and Luthi, S. M., 1988. Borehole electrical images in the Basement of the Cajon Pass scientific drill holes, California; fracture identification and tectonic implications. *Geophys. Res. Lett.*, 15(9):1021–1024.

Presley, B. J., 1971. Techniques for analyzing interstitial water samples. Part 1: determination of minor and major constituents. *In* Winterer, E. L., Riedel, W. R., et al., *Init. Repts. DSDP*, 7(Pt. 2): Washington (U.S. Govt. Printing Office), 1749–1755.

Rust, C. F., 1952. Electrical resistivity measurements on reservoir rock samples by the two-electrode and four-electrode methods. *Trans. Am. Inst. Mining Metall. Engrs.*, 195:217–224.

Sayles, F. L. , Manheim, F. T., and Waterman, L. S., 1973. Interstitial water studies in small core samples, Leg 15. *In* Heezen, B. C., MacGregor, I. D., et al., *Init. Repts. DSDP*, 20: Washington (U.S. Govt. Printing Office), 783–804.

Schlager, W., and James, H. P., 1978. Low-magnesian calcite limestones forming at the deep-sea floor, Tongue of the Ocean, Bahamas. *Sedimentology*, 25:675–702.

Schlumberger, Inc., 1972. *Log Interpretation: Vol. 1, Principles*: New York (Schlumberger).

Serra, O., 1984. *Fundamentals of Well Log Interpretation: Vol. 1. The acquisition of Logging Data*: Amsterdam (Elsevier).

Shepard, F. P., 1954. Nomenclature based on sand-silt-clay ratios, *J. Sediment. Petrol.*, 24:151–158.

Shipboard Scientific Party, 1987. Site 645. *In* Srivastava, S. P., Arthur, M. A., et al., *Proc. ODP, Init. Repts.*, 105: College Station, TX (Ocean Drilling Program), 61–418.

Solorzano, L., 1969. Determination of ammonia in natural waters by phenol-hypochlorite method. *Limnol. Oceanogr.*, 17:799-801.

Strickland, J.D.H., and Parsons, T. R., 1968. A manual for seawater analysis. *Bull. Fish. Res. Bd. Can.*, 167:311.

Timur, A., and Toksoz, M. N., 1985. Fundamentals of well log interpretation. *Annu. Rev. Earth Planet. Sci.*, 13:315–344.

Vacquier, V., 1985. The measurements of thermal conductivity of solids with a transient liner heat source on the plane surface of a poorly conducting body. *Earth Planet. Sci. Lett.*, 74:275–279.

van Morkhaven, F.P.C.M., Berggren, W. A., Edwards, A. S., et al., 1986. Cenozoic cosmopolitan deep-water benthic foraminifera. *Mem. Cent. Rech. Explor. Prod. Elf Aquitaine, 11.*

Von Herzen, R. P., and Maxwell, A. E., 1959. The measurements of thermal conductivity of deep-sea sediments by a needle probe method. *J. Geophys. Res.*, 64:1557–1563.

Wentworth, C. K., 1922. A scale of grade and class terms for clastic sediments. *J. Geol.*, 30:377–392.

Ms 133A-102